CAP DE CREUS CANYON: A LINK BETWEEN SHELF AND SLOPE SEDIMENT DISPERSAL SYSTEMS IN THE WESTERN GULF OF LIONS, FRANCE

A Thesis

by

AMY LOUISE DEGEEST

Submitted to the Office of Graduate Studies of
Texas A&M University
in partial fulfillment of the requirements for the degree of

MASTER OF SCIENCE

December 2005

Major Subject: Oceanography

CAP DE CREUS CANYON: A LINK BETWEEN SHELF AND SLOPE SEDIMENT DISPERSAL SYSTEMS IN THE WESTERN GULF OF LIONS, FRANCE

A Thesis

by

AMY LOUISE DEGEEST

Submitted to the Office of Graduate Studies of
Texas A&M University
in partial fulfillment of the requirements for the degree of

MASTER OF SCIENCE

Approved by:

Chair of Committee, Beth L. Mullenbach
Committee Members, Wilford D. Gardner
Brian J. Willis
Head of Department, Wilford D. Gardner

December 2005

Major Subject: Oceanography

ABSTRACT

Cap de Creus Canyon: A Link Between Shelf and Slope Sediment Dispersal Systems in the Western Gulf of Lions, France. (December 2005)

Amy Louise DeGeest, B.S., University of Washington; B.S., University of Washington

Chair of Advisory Committee: Dr. Beth Mullenbach

Previous work in the Gulf of Lions, France has suggested that significant amounts of sediment may be escaping through the western part of this tectonically passive margin, despite it being far-removed from the primary sediment source (the Rhone river, ~160 km to the NE). It is hypothesized that the westernmost Cap de Creus canyon is intercepting the regional sediment-transport pathway and directing it offshore, allowing significant sediment export through this area. The overall goal of this project is to determine pathways and causes of sediment movement into Cap de Creus canyon to determine its role in off-shelf sediment export within the Gulf of Lions.

Box cores were collected within the canyon and on the adjacent shelf on five cruises (2003-2005). Geochronology (^{210}Pb-derived accumulation rates), grain-size distributions, and sedimentary structures (x-radiography) were analyzed to assess sedimentation patterns. Results indicate two mid-depth shelf depocenters (30-90 m water depth) separated by a zone of bypassing created by current acceleration around a headland. Within the canyon, the northern flank and mid-depth thalweg are modern depocenters of fine-grained sediments. The canyon head and southern flank are considered non-depositional for fine grains, although the head may be accumulating

sands. Material enters the canyon from the northern rim (via advection of shelf benthic nepheloid layers), the southern rim (via dense-water cascading off the shelf), and through the canyon head (primarily coarse-grains). Budget calculations indicate that 9-23% of the sediment input to the Gulf is sequestered on the shelf and 1-4% is accumulating in upper Cap de Creus canyon. An ephemeral mud layer within the canyon axis indicates rapid deposition and frequent flushing, suggesting that sediment is moving through the upper canyon. This is also supported by high suspended-sediment concentrations associated with off-shelf dense-water flows. This study suggests that Cap de Creus canyon is an important conduit of sediment past the shelf break and the western margin is a primary location of sediment export from the Gulf of Lions.

ACKNOWLEDGMENTS

This research would not have been possible with the continued guidance and support of my advisor, Dr. Beth Mullenbach. Throughout cruises, meetings, and lab work, she has continually proven herself to be a talented educator and trustworthy mentor. My committee (Dr. Wilf Gardner and Dr. Brian Willis) has also always been helpful, offering guidance and assistance as needed through the research project.

I would like to thank my collaborating scientists as well: Pere Puig, Xavier Durrieu de Madron, Dan Orange, Ana Garcia-Garcia, Mike Field, Serge Berne, Tina Lomnicky, and particularly Chuck Nittrouer, who has supported me and guided me throughout my education. Also, the captains and crews of the R/V Tethys II, R/V Oceanus, and R/V Endeavor deserve a sincere note of appreciation.

Finally, the most important people have always been my friends and family. My parents (Rod and Carol) and sister (Susie) have never stopped believing in me and have always been there for me, no matter what happens. Zach, who has managed to finally make Texas feel a little like home, has provided a welcome and comfortable reprieve from the stresses associated with life in academia. Megan, who has never failed to read my writing (despite always seeing the roughest of drafts), has always been my best friend. Amy, Rachael, and Melissa are always there to share the ups and down of life. Dan and Stevie always listen and understand what its like to be a student far away from home. Derek (in the same state yet so far away) reminds me of how much fun life can be. And finally Jeff, who always tells it like it is and reminds me of what really matters.

TABLE OF CONTENTS

LIST OF FIGURES

FIGURE Page

LIST OF TABLES

1. INTRODUCTION AND OBJECTIVES

The same processes that presently move sediment across the continental margin also help to shape the margin over longer timescales (e.g. Walsh and Nittrouer, 2003; Nittrouer, 1999). Different mechanisms of sediment transport create distinct margins: hemipelagic sedimentation builds slowly outward over time; whereas gravity flows erode submarine canyons and channels, making margins bathymetrically complex (Canals et al., 2004). The relationship between modern sediment deposition and longer-timescale margin features indicate the importance of short-timescale processes in forming the longer-term geologic record (Nittrouer and Kravitz, 1996).

The amount of fluvial sediment that escapes to the deep-sea has long been known to be partially controlled by sea-level fluctuations and the resulting amount of submerged continental shelf and estuarine volume (Broecker et al., 1958). During the present sea-level highstand, 70% of the shelf area is covered with relict sediment and significant amounts of modern terrigenous sediment is confined to estuaries or trapped on broad continental shelves (Emery, 1968). Although modern sediment accumulation past the shelf break (i.e. the slope and deep-sea) has been observed in many locations, rates are typically low and the primary mechanism of escape is generally nepheloid layer advection off the shelf break or erosion within the canyon (Gardner; 1989; Baker and Hickey, 1986; Carson et al., 1986).

Contrary to this premise, recent studies have shown that significant amounts of sediment can escape the shelf break during sea-level highstands by other methods, such

---

This thesis follows the style of Marine Geology.

as gravity-driven sediment flows (Puig et al., 2004; Mullenbach et al., 2004; Walsh and Nittrouer, 2003). Tectonically-active margins, which receive a large fraction of the global sediment load due to their steep terrains proximal to the coast, allow significant sediment escape where fluvial sediment input passes onto narrow shelves (Mullenbach et al., 2004; Walsh and Nittrouer, 2003; Kineke et al., 2000; Milliman and Syvitski, 1992). Thus, large volumes of sediment may reach the deep sea during highstands in sea level; however, the range of margin characteristics that permit sediment export from the continental shelf have not been completely explored.

The sedimentary link between the continental shelf and slope controls the degree of sediment escape during highstand conditions. Submarine canyons have been identified as a prominent and efficient link between the shelf and slope systems (Walsh and Nittrouer, 2003; Liu et al., 2002; Kineke et al., 2000; Mullenbach and Nittrouer, 2000; Sanchez-Cabeza et al.., 1999; Puig and Palanques, 1998; Durrieu de Madron, 1994; Baker and Hickey, 1986). Canyons, which can substantially reduce the width of the shelf as well as intercept sediment transport patterns, are ideal pathways of sediment export past the shelf break (Paull et al., 2003; Granata et al.. 1999; Gardner, 1989). Canyons on active margins adjacent to large sediment sources are especially efficient in the transfer of sediment, due to the formation of gravity-driven flows often created by sediment loading (e.g. Kineke et al., 2000). In contrast, nepheloid layer advection is usually dominant in canyons on wide passive margins. This transport is enhanced relative to the open slope but is much reduced compared to their active-margin counterparts (Carson et al., 1986).

The Gulf of Lions, France is a wide, passive continental margin (Fig. 1). Contrary to the currently accepted paradigm of sediment trapping on passive margins, this margin appears to have significant off-shelf sediment escape at locations distal to the primary sediment source (the Rhone river) during the present sea level high-stand (Frignani et al., 2002; Durrieu de Madron, 1994; Durrieu de Madron et al., 1990; Courp and Monaco, 1990; Got and Aloisi, 1990). Previous studies have shown that Rhone sediment (2-5 x 10^6 tons $year^{-1}$) is either deposited on a prodelta or dispersed along the coast by regional currents; sediment does not reach the shelf break in the vicinity of the river mouth (Got and Aloisi, 1990; Arnau et al., 2004). However, regional current patterns suggest a funneling of sediment towards the southwest portion of the Gulf where the shelf narrows (due to the presence of a headland) and is incised by Cap de Creus Canyon (Durrieu de Madron, 1990). This canyon directly intercepts the regional southwestward current and is situated to be a primary conduit of sediment escape past the shelf break for sediment from the entire Gulf of Lions shelf system, including Rhone river sediments. If sediment is escaping in significant quantity in the western Gulf of Lions, this region will give insights into sedimentation processes on modern passive margins and margin evolution.

Based on previous studies and preliminary work, Cap de Creus canyon is hypothesized to be a primary outlet of sediment for the entire Gulf of Lions region and an active conduit for sediment to the deeper continental slope. The null hypothesis is that Cap de Creus canyon does not show any evidence of active transport beyond the expected, low-concentration nepheloid layers. This research focused on upper Cap de

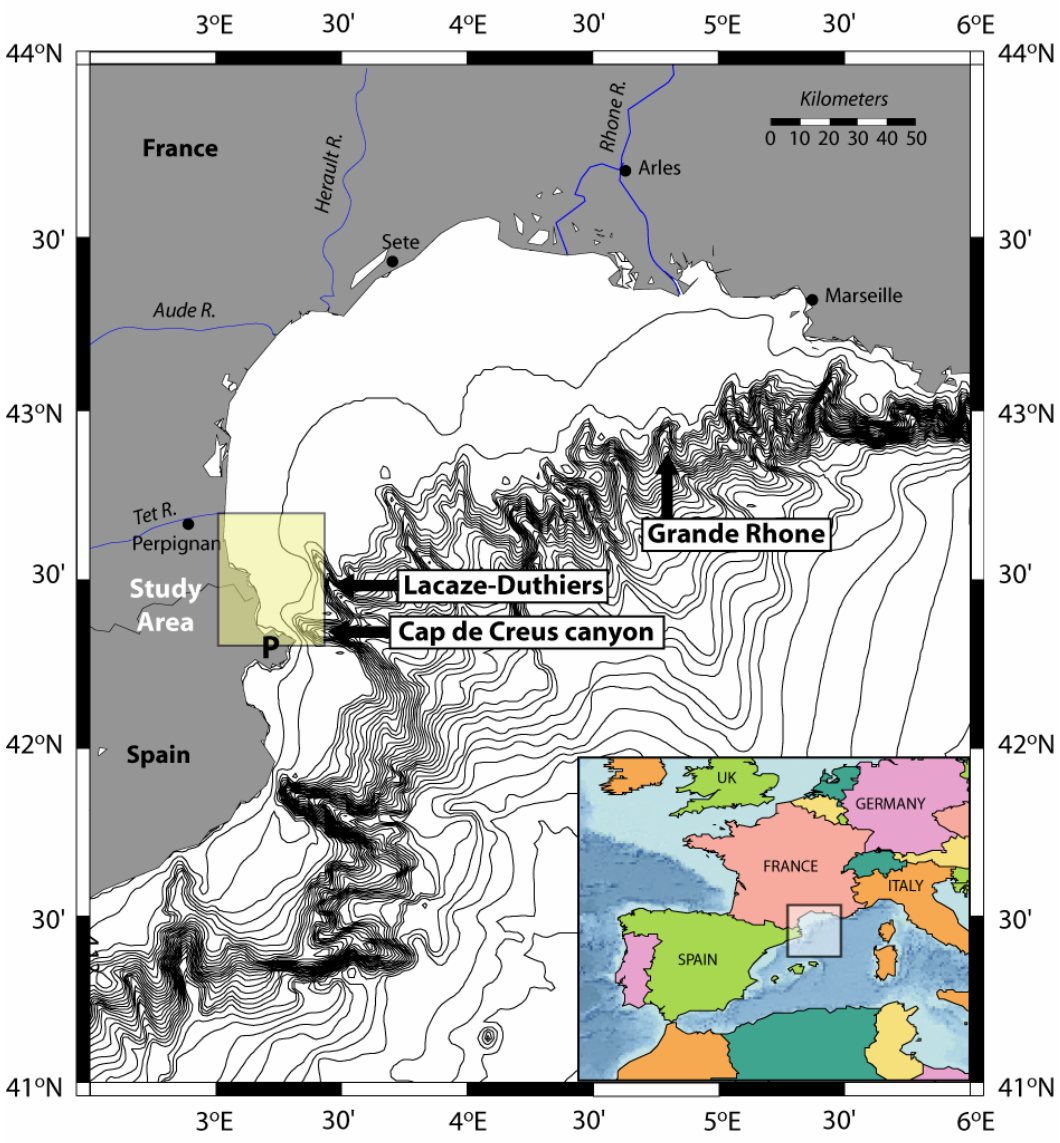

Figure 1. General map of the Gulf of Lions. Study area outlined by the yellow box. Cap de Creus promontory is denoted by **P**.

Creus canyon (>780 m thalweg water-depth) and the adjacent shelf with the following objectives: (1) locate modern depocenters on the western Gulf of Lions shelf and in Cap de Creus canyon; (2) identify conduits of sediment movement from the shelf to the deep slope system by combining information on sedimentation patterns and morphology; and (3) infer the primary mechanism moving sediment off the continental shelf and into the canyon. The results offer a greater understanding of the shelf-slope link in the western Gulf of Lions as it is facilitated by Cap de Creus canyon; this information will aid in the identification of important, active sedimentary processes and the interpretation of strata formed during the present highstand in sea-level.

2. REGIONAL SETTING

2.1 Geologic Setting

Extending from the Pyreanean mountains of northern Spain to the Alps of eastern France, the Gulf of Lions is a passive margin that shows little tectonic influence (Berne et al., 2004). It initially formed by Oligocene-Aquitanian rifting followed by the formation of a micro-ocean separating the Corsica-Sardinia block from the French margin (Berne and Gorini, 2005). Predominantly underlain by thick Messinian evaporites, the margin is dominated by complex pressure deformation structures overlain by a relatively thin Holocene sediment layer (Canals et al., 2004). The Gulf of Lions continental shelf reaches a maximum width of 72 km (near the mouth of the Rhone), and narrows westward to less than 15 km near Cap de Creus Canyon (Fig. 1).

The shelf-break has complex bathymetry, as it is incised by at least twelve submarine canyons that coalescence into two primary channels on the deep slope (Canals et al., 2004). Some of these canyons extend relatively far onto the shelf (i.e. Cap de Creus and Lacaze-Duthiers canyons in the western Gulf), while others initiate much farther from shore (i.e. Grand and Petit Rhone in the eastern Gulf). Although the origin of these canyons is still debated, a recent study suggests that they formed as a result of halokinesis-derived depressions above Messinian evaporates, which were then enhanced by turbidite erosion and mass-wasting (Canals et al., 2004). The emplacement and path of Cap de Creus canyon was also partially controlled by seaward extensions of land-based structural lineaments (Canals et al., 2004). Extensive seismic studies by Baztan et al. (2004) and Baztan et al. (2005) support that the canyons are erosional features,

although he also suggests that some of the canyons may have been enhanced by tubidity-current erosion of axial incisions, making the main-canyons more susceptible to failures. Cap de Creus and Lacaze-Duthiers canyons, which lack this axial incision within the canyon head, do not fit this profile.

The Rhone River (the main source of sediment to the Gulf of Lions) has a mean water discharge of 1,700 m^3 sec^{-1} (Arnau et al., 2004). The associated freshwater plume, deflected southwestward by the general current flow, funnels sediment along the coastline (Arnau et al., 2004). The Rhone provides 2.2-5 x 10^6 tons of sediment per year, which is equivalent to approximately 80% of the total sediment input to the region (Zuo et al., 1991; Courp and Monaco, 1990). A significantly higher value (10 x 10^6 ton $year^{-1}$) for sediment discharge was previously reported by Milliman and Meade (1983). Martin et al (1989) suggested that only 10% of Rhone river sediment escape to the open Mediterranean Sea, while the rest is sequestered in estuaries and on the continental shelf. This value is based only upon limited sediment-trap data focused primarily in the eastern canyons, suggesting that they may have disregarded significant amounts of sediment escaping from the western margin.

The remainder of the Holocene sediment supplied to the Gulf of Lions comes primarily from six smaller rivers (i.e. the Tet and Aude rivers), which respond quickly to climatic variations with episodic discharges that are difficult to quantify (Certain et al., 2005). Consequently, little data exists on the annual sediment and water discharge of these rivers. A small fraction of sediment is also supplied by biological production and atmospheric deposition of Saharan dust (Wegrzynek et al., 1997).

Previous research has identified a Holocene formation on the shelf commonly referred to as the "Epicontinental Prism" (Jago and Barusseau, 1981; Martin, 1981). This prism, the result of repeated changes in sea-level, is underlain by a layer of basal, transgressive Pleistocene sands (Certain et al., 2005). These sands are overlain by modern sands in the near-shore environment (0-30 m water depth) and modern muds at mid-shelf depths (~30-80 m), but are exposed on the outer shelf (Courp and Monaco, 1990; Certain et al., 2005). The near-shore sands are frequently overshadowed by small prodeltas that form at the mouths of the smaller western rivers and the sizeable delta created by the Rhone river (Courp and Monaco, 1990).

Zuo et al (1991 and 1997) reported ^{210}Pb-derived sedimentation rates of 0.1 to 0.6 cm yr^{-1} in the Gulf of Lions, with the highest rates being just west of the Rhone river mouth and the lowest being on deep-slope interfluves and in the deep-sea. They estimate that $10 \pm 4 \times 10^6$ tons of sediment is deposited on the margin each year, the majority of which is supplied by the Rhone river (Wegrzynek et al., 1997). Courp and Monaco (1990) previously reported accumulation rates (based on ^{210}Pb and ^{14}C dating) ranging 0.16 to 2.9 g m^{-2} day^{-1} on the margin, which corresponds to sedimentation rates of 0.04 to 0.8 mm/yr, assuming a bulk density of 1.32 g/cm^3. These estimates appear to be based primarily on slope cores.

Previous studies also have suggested that sediment may be escaping the shelf via submarine canyons. The Grand Rhone canyon (located adjacent to the Rhone river), and Lacaze-Duthiers canyon (located northeast of Cap de Creus canyon) have both been shown to be preferential conduits for off-shelf sediment transport from the Gulf of

Lions: enhanced suspended sediment concentrations within their boundaries suggest a funneling of sediment within these canyons (Durrieu de Madron, 1994; Monaco et al., 1999). Suspended sediment concentrations and seaward sediment fluxes within the canyons have been found to increase westward, suggesting that the western part of the Gulf may act as the primary outlet of sediment for the entire Gulf of Lions (Monaco et al., 1999).

Within Lacaze-Duthiers canyon, Courp and Monaco (1990) identified two zones of accumulation: the upper canyon (between 400 and 1100 m) traps hemipelagic material from the shelf, while the upper fan accumulates sediments transported by turbidites. These combine for a total sedimentary budget of ~26 x 10^3 tons of lithogenic sediment accumulating annually within Lacaze-Duthiers canyon. Mineralogical evidence suggests that Rhone river sediments reach this western canyon and therefore may escape the shelf at this distal location (Frignani, 2002). Courp and Monaco (1990) also showed that 70% of the particulate flux entering Lacaze-Duthiers canyon passes through the canyon to the deep sea on the <100-year timescale, suggesting that these canyons are efficient conduits of sediment past the shelf edge.

Most previous studies are focused on the eastern half of the margin due to the prominence of Rhone sediments. Almost all work in the western Gulf has focused on Lacaze-Dutheirs Canyon; the role of the western shelf and Cap de Creus Canyon (the westernmost canyon) in off-shelf sediment export has not yet been extensively explored.

2.2 Oceanographic Setting

The Gulf of Lions is a wave-dominated, microtidal environment with an average tidal of range of less than 0.25 m (Certain et al., 2005). The general circulation pattern within the Gulf is dominated by the Liguro-Provencal-Catalan (LPC) or Northern current, which flows southwestward along the shelf break (Fig. 2). It enters the Gulf via the Liguran Sea to the east and moves at speeds up to 50 cm/s towards the Catalan margin, off the coast of Spain (Millot, 1990). This flow creates an overall east-to-west circulation along the outer portions of the shelf, suggesting that sediment transport patterns will also generally be westward (Durrieu de Madron, 1990). This current shows a clear seasonality: its flux tends to be double in winter (a period of heighted sediment input) relative to summer (Millot, 1990). Meanders of this current frequently move onto the shelf and establish a large, anti-cyclonic gyre in the Gulf, due either to eddy formation or the influence of northwesterly winds (Millot, 1990). This is frequently associated with Tramontane (northwesterly) winds that agitate the waters and create significant wave energy, thereby initiating a period of heightened sediment transport towards the southwest within the Gulf of Lions (Millot, 1990; Arnau et al., 2004). It is during these particular conditions, most commonly experienced in spring, that we expect to see the greatest amount of sediment movement on the shelf and possibly past the shelf break.

These northwesterly winds are also responsible for dense-water formation in winter on the Gulf of Lions continental shelf. Wind-cooling of upwelled saline waters causes an increase in density, the water sinks to a level of neutral buoyancy, establishing

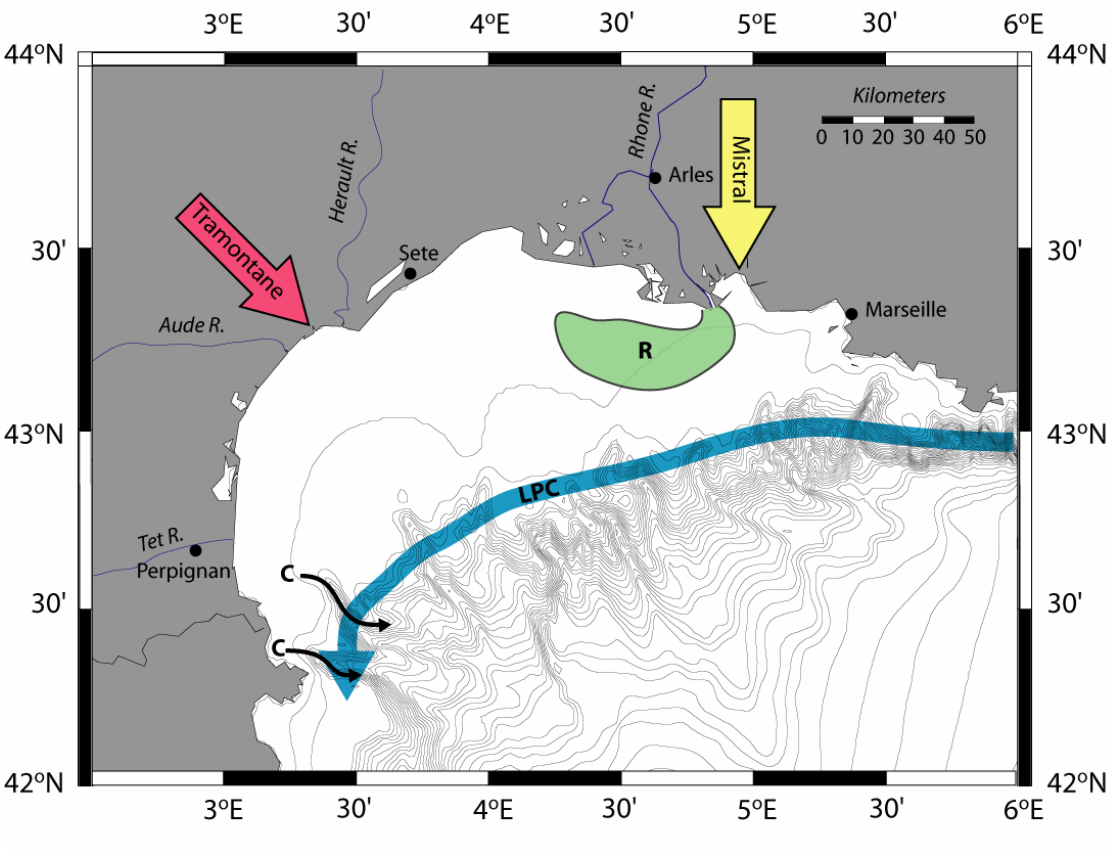

Figure 2. Regional physical oceanography of the Gulf of Lions. The Liguro-Provencal-Catalan current is shown in blue; Rhone plume shown in Green; different wind regimes shown by pink and yellow arrows. C denotes areas of dense-water formation and cascading (only shown in western gulf, but does occur elsewhere on the shelf). Modified from Arnau et al. (2004) and Millot (1990).

unique thermohaline circulation within the Gulf (Millot, 1990). Durrieu de Madron (2004) reported that these waters tend to pool on the outer shelf until they eventually cascade down the slope as a near-bottom, water-driven gravity flow, acting as a possible mechanism of escape for resuspended sediment. These cascades have been identified in both Lacaze-Duthiers and Cap de Creus canyons, suggesting that they may be primary mechanism of moving sediment into the canyons (Durrieu de Madron, 2005).

Interactions of the LPC current with the complex bathymetry of the Gulf of Lions shelf break also can create conditions for off-shelf sediment transport. The current impinges on the canyons at nearly right angles (due to its along-slope flow), generating up- or down-canyon currents (Millot, 1990). Combined with the movement of the LPC current, this up- and down-canyon circulation creates favorable conditions to move sediment off the continental shelf. The dominance of these currents relative to others is presently unknown.

3. METHODS

3.1 Sample Collection

Sampling was conducted on five cruises in the western Mediterranean onboard the R/V Tethys II, R/V Oceanus, and R/V Endeavor (Figs. 3 and 4). Although the initial cruises (November 2003 and March 2004) focused on sampling within the canyon thalweg, space samples from the shelf established a framework for continued work. The third cruise (October 2004) involved extensive sampling within the canyon thalweg and on the northern flank, as well as on the shelf adjacent to the canyon head. The final two cruises (February and April 2005) focused primarily on higher-resolution grid sampling of southern shelf and near the coastal promontory, as well as sampling the southern flank of Cap de Creus canyon. Sites having deposits indicative of active sediment flow, such as storm layers or fluid muds, were reoccupied on multiple cruises to allow for temporal comparison and identification of seasonal features.

Samples were collected using a spade box corer (20 x 30 cm footprint, 60 cm depth) to allow for minimal disturbance of the sediment-water interface. Once on deck, cores were subsampled into 1 cm intervals and stored for lab analysis. X-radiographs were also taken to visualize sedimentary structures and significant grain size layering.

3.2 Laboratory Methods

Three types of laboratory analyses were performed on each core sample: alpha spectroscopy, gamma spectroscopy, and granulometric analysis.

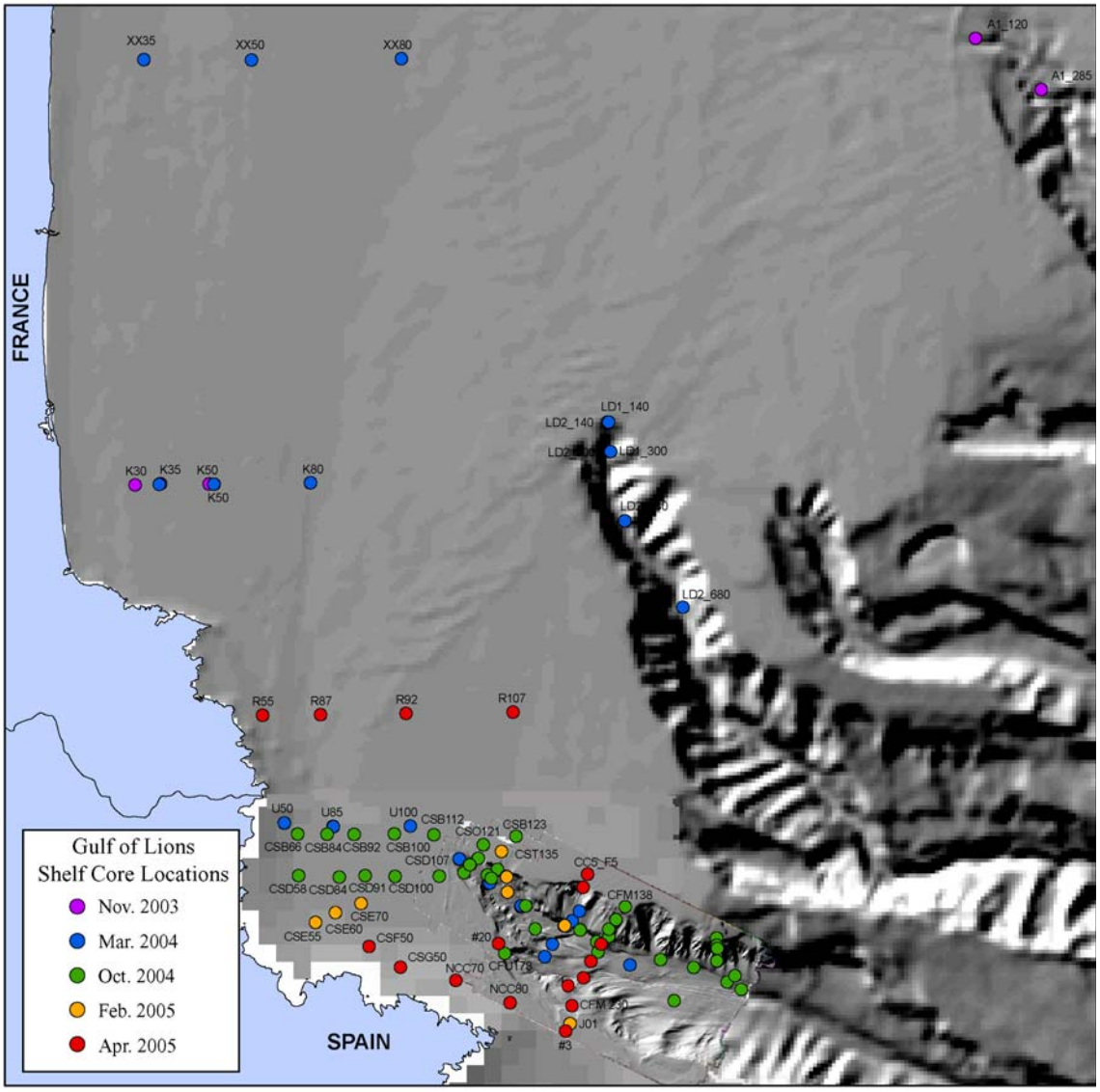

Figure 3. Shelf core locations. Symbol color designates cruise during which a core was collected. Canyon cores are not labeled to save space.

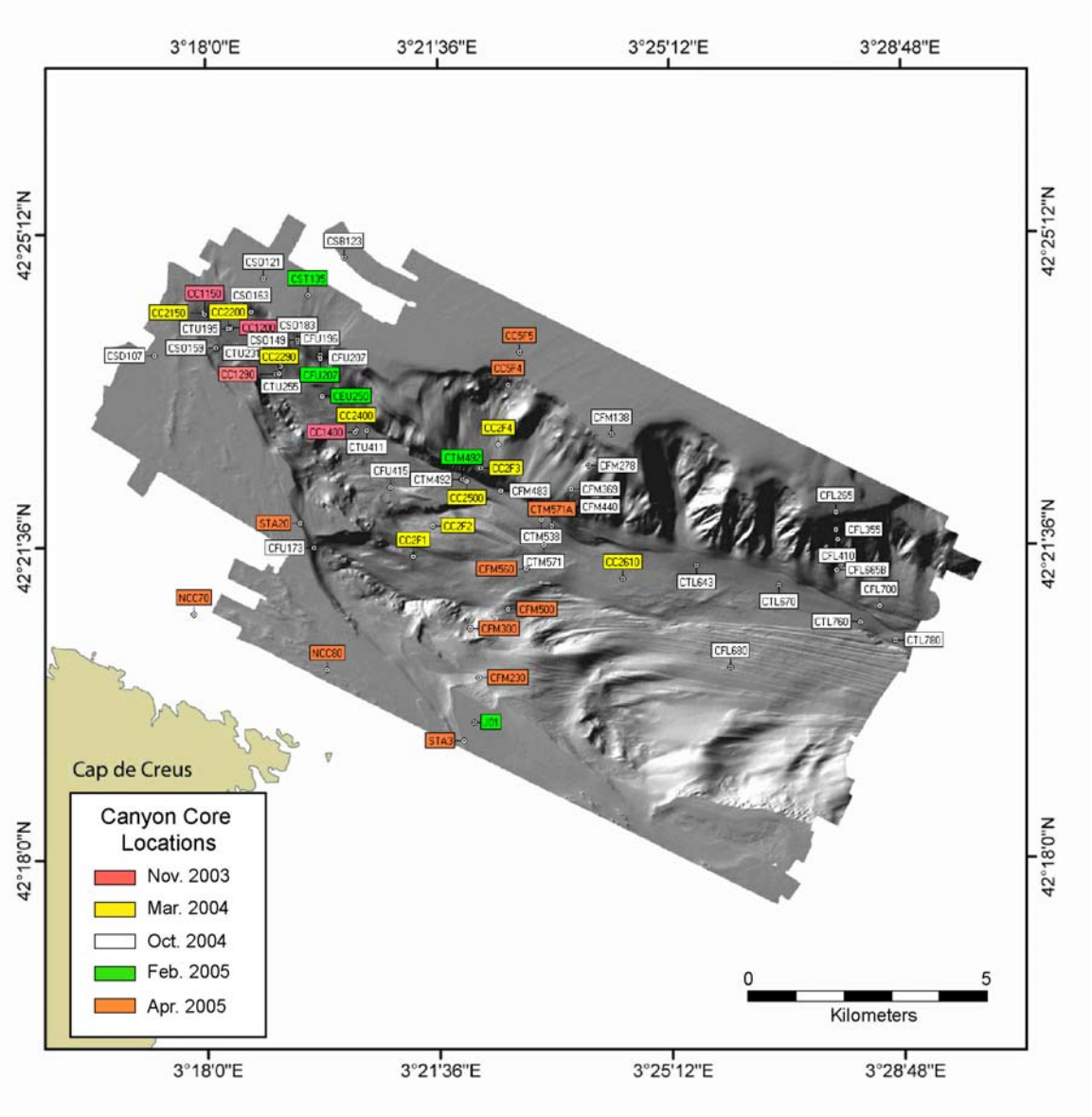

Figure 4. Canyon core locations.

3.2.1 Alpha Spectroscopy

Accumulation rates over a 100-year timescale were calculated using the decrease of ^{210}Pb activity with depth in the seabed as determined by alpha spectroscopy. Part of the ^{238}U decay series, ^{210}Pb (half-life = 22.3 yrs) is supplied to the oceans by terrestrial run-off, atmospheric precipitation, and the decay of ^{226}Ra in the water column. Coastal waters, which can be quickly depleted of ^{210}Pb due to high-sediment concentrations, are generally kept at constant values of ^{210}Pb by on-shore advection of deep water, which have a greater supply of ^{210}Pb.

Once dissolved in the seawater, ^{210}Pb is highly particle-reactive and will be scavenged by sediment particles as they sink though the water column. It has a residence time of less than one year in the nearshore marine water column due to adsorption onto particles, and is chemically immobile once it is deposited in the sediment (Nittrouer et al., 1979). When sediment is buried in the seafloor, the particle activity begins to decay; therefore, the rate of decrease in activity with depth (due to isotopic decay) from the sediment-water interface acts as a measure of accumulation rates at each specific location. A mean supported ^{210}Pb activity is present in all sediments, regardless of age, due to new production created by the decay of ^{226}Ra in sediments.

To calculate accumulation rates, supported values are subtracted from the total activity to determine the excess activity of sediments at each depth interval. Assuming the rate of biological mixing is negligible relative to the rate of sediment accumulation, the exponential decrease of excess ^{210}Pb activity ($^{210}Pb_{xs}$, the activity attained while sinking through the water-column) with depth is used to calculate an accumulation rate:

$$A = \frac{-\lambda \cdot z}{\ln\left(\frac{C_z}{C_o}\right)}$$

where A is the accumulation rate, λ is the decay constant for ^{210}Pb (0.693/half-life), z is the depth in the seabed, C_o is the excess activity at the sediment-water interface, and C_z is the excess activity at depth z (Nittrouer et al., 1979; Mullenbach, 2002). These accumulation rates are average rates based on the assumption of steady-state deposition over a 100-year timescale.

Localized lowered activities that do not follow the typical steady state exponential decrease with depth can either be due to grain-size differences or supply limitation of dissolved ^{210}Pb. ^{210}Pb preferentially adsorbs to finer grains due either to surface coatings or greater available surface areas, so down-core variability in grain-size can result in apparent variability of ^{210}Pb activity. Coastal waters can have periods with high particle concentrations that absorb the isotope more quickly than it can be supplied to the system (primarily by onshore advection), which could also cause ^{210}Pb variability in the seabed (Sommerfield et al., 1999; Sommerfield and Nittrouer, 1999). It is important to note that the activity of ^{210}Pb indicates sediment interaction with the water column and can represent resuspended sediments as well as fresh input from fluvial sources (Nittrouer et al., 1979). Other methods must be used to distinguish between resuspended sediments and recent fluvial sediments.

Laboratory analysis of ^{210}Pb activities was conducted following the methods of Nittrouer et al (1979). Samples were spiked with a ^{209}Po tracer, leached with Nitric and Hydrochloric acids, plated onto silver planchets, and counted for relative alpha decay of

^{209}Po and ^{210}Po over a 24-hour period on a Canberra Alpha Analyst alpha detector. ^{210}Po, which is assumed to be in secular equilibrium with ^{210}Pb, was used because it is easier to determine the activity of this isotope relative to ^{210}Pb (Nittrouer et al., 1979). Samples that have large fractions of sand or shell fragments were treated similarly to muddy samples; however very large, articulated shells or wood fragments (anything that would not behave similarly to the ambient sediments) were removed prior to analysis. In order to account for down-core grain size variations, total activities were normalized to the percent of clay in each sample interval. Sandy layers that exhibited little ^{210}Pb variation down core were simply classified as recent (within the last 100 years) or relict (older than 100 years) based on the presence or absence of $^{210}Pb_{xs}$ activities, respectively.

3.2.2 Gamma Spectroscopy

Select samples were dried and analyzed by gamma spectroscopy at the University of Washington on Canberra Low Energy Germanian (LEGe) detectors. Analysis focused on ^{7}Be (half life = 53.3 days, photopeak = 478 keV), a highly particle-reactive cosmogenic radioisotope that generally reaches the marine system by terrestrial run-off and fluvial input (Larsen and Cutshall, 1981; Olsen et al., 1985; Bettoli et al., 1995). Its presence indicates sediments that have entered the marine system from fluvial sources in the past 3-4 months and therefore it is a useful indicator of recent fluvial influxes. A lack of detectable ^{7}Be in core samples could indicate that (1) sediments are trapped on other regions of the shelf for ≥4 months before they move to the shelf edge, allowing the ^{7}Be-labeled sediment to decay to below-detectable levels of activity or (2)

the fluvial inputs are no longer tagged with ^{7}Be when they enter the marine system due to long particle residence times in the river basins.

3.2.3 Granulometric Analysis

Grain-size results were used to remove grain-size effects from isotopic measurements and to create distribution maps of grain size variations. Samples were disaggregated using a 0.05% (by weight) solution of sodium metaphosphate and an ultrasonic bath. Each sample was then wet-sieved at 63 μm to isolate sand and coarser materials from finer fractions. All material that passed through the sieve was analyzed using a Sedigraph 5100 particle size analyzer to determine the distributions of silt- and clay-sized particles. The total fine faction was then dried, weighed, and combined with the sand fraction to determine percent sand, silt, and clay by weight. These percentages were then used to classify sediments following the scheme outlined in Table 1.

3.2.4 Ancillary Data

Collaborating scientists have provided data essential to this project. High-resolution multibeam bathymetry of Cap de Creus Canyon was acquired, processed, and provided by Fugro Survey Ltd. and AOA Geophysics Inc. Data were acquired with Fugro's M/V Geo Prospector, equipped with a Simrad EM300 hull-mounted multibeam system (1x1 degree) and a GeoAcoustics 534A 4x4 hull-mounted sub-bottom profiler. Gulf of Lions regional multibeam bathymetry was supplied by S. Berne (IFREMER) and P. Puig. (Berne et al., 2002). Hydrographic time-series (currents, suspended sediment

Table 1. Definition of grain-size classifications.

Classification	*Description*
Gravel	Consolidated mud or sand with significant amount of gravel[1]
Sand	>75% sand[2] <25% silt[3] + clay[4]
Silty sand	>80% sand + silt, more sand than silt <20% clay
Sandy Mix	Sand-silt-clay = more highest percentage of sand 20 - 60% sand, 20 - 60% silt, 20 - 60% clay
Clayey-sand	>80% sand + clay, more sand than clay <20% silt
Silty Mix	Sand-silt-clay = more highest percentage of silt 20 - 60% sand, 20 - 60% silt, 20 - 60% clay
Clayey Mix	Sand-silt-clay = more highest percentage of clay 20 - 60% sand, 20 - 60% silt, 20 - 60% clay
Clayey-silt	>80% silt + clay, more silt than clay <20% sand
Silty-clay	>80% silt + clay, more clay than silt <20% sand

[1]Gravel = > 2 mm
[2]Sand = 0.0625 - 2 mm (63 – 2000 μm)
[3]Silt = 0.004 – 0.0625 mm (4 – 63 μm)
[4]Clay = <0.004 mm (<4 μm)

concentrations, temperature) from moorings and tripods located from 145-750 m water-depth in the canyon was available from P. Puig and A. Palanques. ADCP data of regional currents and circulation patterns were provided by X. Durrieu de Madron. Seismic chirp lines on the shelf and canyon were used courtesy of Mike Field and Pat Hart at the United States Geological Survey. These data were acquired using an Edgetech 512 Subbottom Profiling System and recorded using Delph Seismic software. Acquisition parameters for the production lines were a 500 – 7200 Hz, 30 ms chirp sweep, 12.5 kHz sampling.

3.3 Data Analysis

Grain-size and accumulation-rate data were plotted onto the high-resolution bathymetry using ArcMap™ to allow for direct comparison of seabed data with detailed morphology. This permitted characterization of specific sub-area types in the canyon based on observed sedimentation patterns and morphologic features. These sections were then classified as depositional, erosional, or areas of bypassing, and were used to evaluate various mechanisms of sediment movement into the canyon (e.g., down-canyon flows versus advective nepheloid layer transport). To place further constraints on the forces instigating sediment movement and accumulation within the western Gulf of Lions, the hydrographic data from Spanish and French scientists was compared to these seabed data to (1) determine specific pathways of sediment movement into the canyon and (2) correlate areas of deposition/bypassing/erosion with hydrographic characteristics. The former offers insights into the origins of sediments escaping the

shelf, while the latter allows the determination of forcing factors moving sediment off of the shelf and into deeper parts of the canyon.

A final objective of this project was to create a semi-quantitative, 100-year timescale budget of sediment accumulating on the western shelf and within upper Cap de Creus canyon. Masses were calculated based on accumulation rates and bulk-densities as determined by this study. Spatial variability in the parameters was roughly estimated based on regional patterns and core characteristics. A difficulty associated with creating a budget was the lack of definitive information pertaining to the total sediment discharged into the Gulf of Lions. The contribution of small, episodic rivers in the western GOL is unknown. Therefore, the budget will be compared to the Rhone river sediment input (as it is the only quantified and most significant source to the Gulf of Lions margin). This semi-quantitative estimate of sediment sequestered by the upper canyon and adjacent shelf will elucidate the role of the western gulf in relation to sediment export from the whole Gulf of Lions.

4. RESULTS

4.1 Gulf of Lions - Western Continental Shelf

The western Gulf of Lions shelf and slope region can be divided into areas based on sedimentary characteristics, oceanographic conditions and seafloor morphology. The continental shelf is separated into three parts: (1) the northwestern shelf (from the northern limit of the study area to Cap Bear), (2) the middle shelf (from Cap Bear to the Spanish-French border), and (3) the southwestern shelf (from the border to Cap de Creus headland) (Fig. 5).

Cap de Creus canyon is divided into four morphological regions: (1) canyon head, (2) thalweg (excluding the canyon head), (3) northern flank and (4) southern flank (Fig. 5). A small part of the southern flank has characteristics similar to the thalweg and is referred to as the near-thalweg southern flank (area 5 on Fig. 5). The portion of the shelf near Cap de Creus canyon is classified as the canyon rim.

4.1.1 Open Shelf

Grain-size results on the continental shelf show patterns similar to those defined by previous studies for the entire Gulf of Lions region (Fig. 6, Table 2). A mid-shelf mud deposit (M.S.M.D), located from approximately 30-85 m water depth, is primarily composed of silty-clays or clayey-silts. Some cores had a fine-sand component (<40% by weight). Cores collected deeper on the shelf (85-130 m) were generally coarse-grained with a significant coarse-sand fraction. Although no cores were collected in water depths shallower than 30 m due to ship limitations, previous

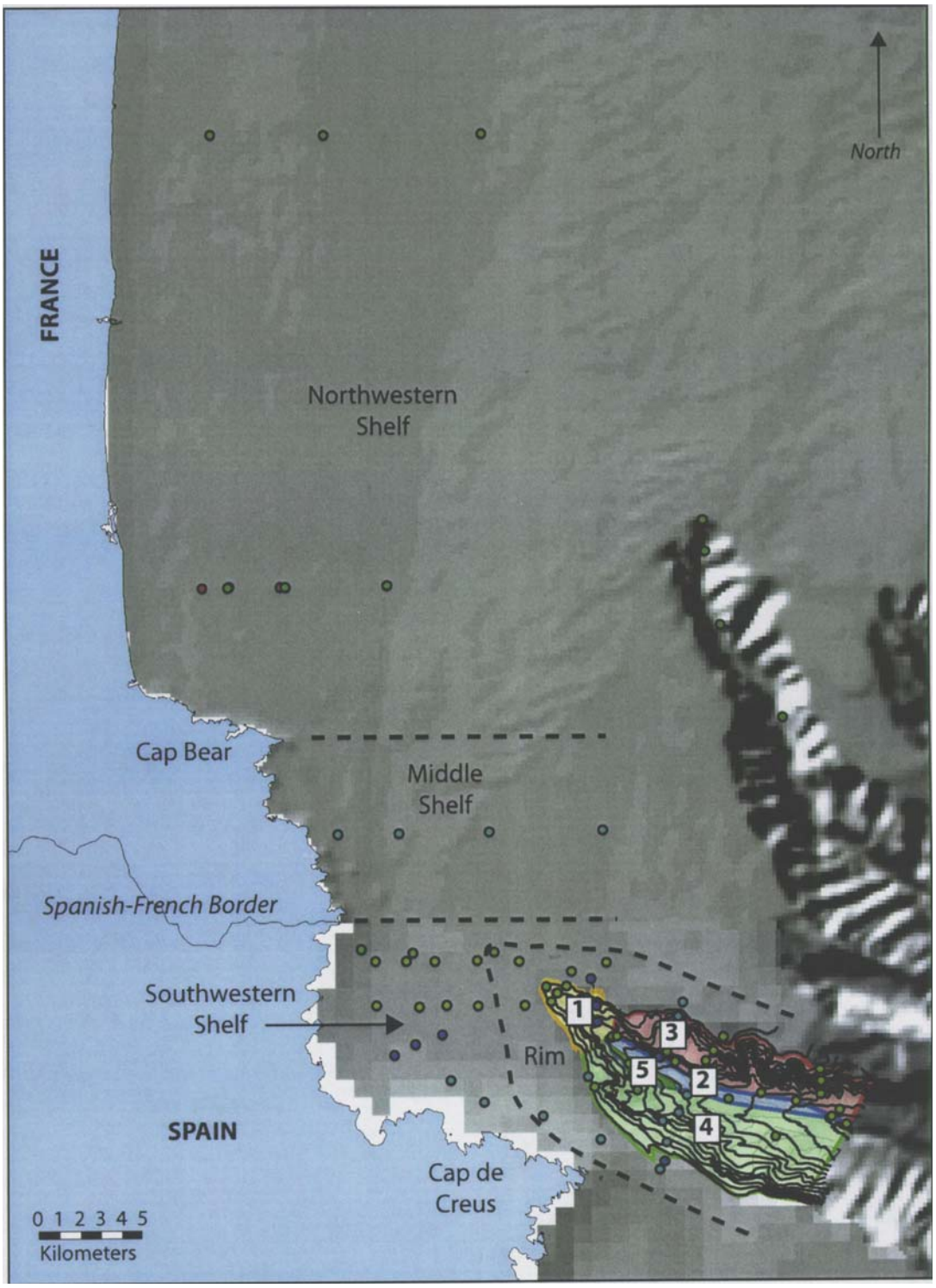

Figure 5. Shelf and canyon physiographic zones. Regions are divided by core characteristics and morphology. Canyon zones area: (1) Canyon head, (2) Thalweg, (3) Northern Flank, (4) Southern Flank, and (5) Near-thalweg southern flank.

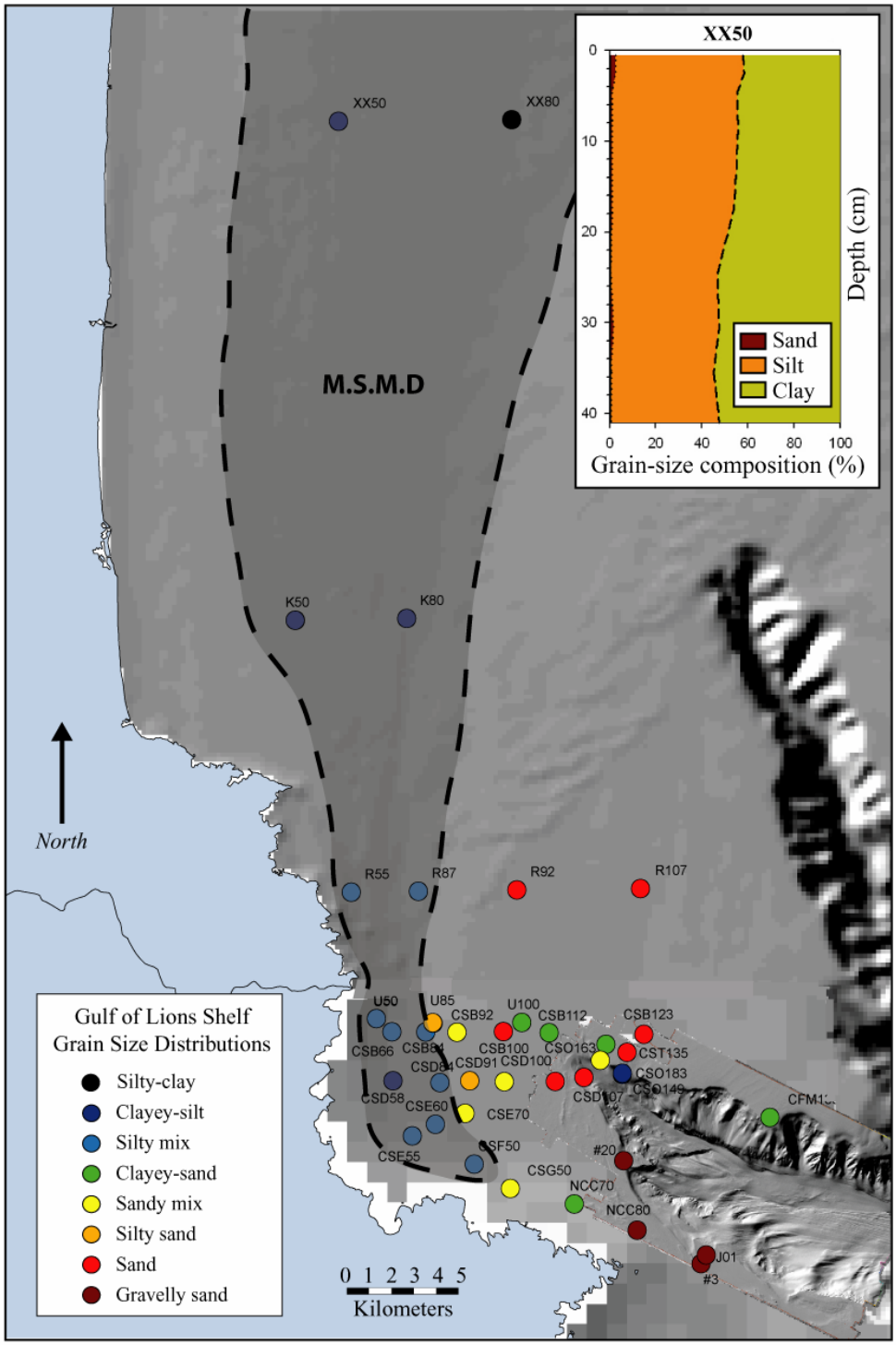

Figure 6. Shelf grain-size distribution with midshelf mud deposit designation. Dark gray area marks the extent of the mid-shelf muds. Inset: example of the minimal down-core variability in grain-size in shelf cores.

Table 2. Shelf core data compilation.

Cruise	*Core*	*Depth (m)*	*Grain Size*	*% sand*	*% silt*	*% clay*	*Accum. Rate (mm/yr)*	*Surf. Activity (dpm/g)*
GOLW04	XX50	50.0	Clayey Silt	2.4	55.4	42.2	1.3	7.8
GOLW04	XX80	79.6	Silty Clay	0.9	44.5	54.6	2	8.7
GOLF03	K50	50.2	Clayey Silt	19.7	54.7	25.7	1	5.7
GOLW04	K50	48.8	Clayey Silt	17.2	53.9	29	1	5.4
GOLW04	K80	79.2	Clayey Silt	3.5	54.9	41.6	2	10.7
EN0405	R55	53	Silty Mix	36.2	37.6	26.2	0.64	4.9
EN0405	R87	90	Silty Mix	34.5	38.5	27	0.56	5
EN0405	R92	95	Sand	80	9.9	10.1	1.1	3
EN0405	R107	113	Sand	89	4.2	6.8	Sand	3.5
GOLW04	U50	51.6	Silty Mix	24.8	46.9	28.3	2.5	5.7
GOLW04	U85	83.6	Silty Sand	62.4	19.8	17.9	0.76	6.1
GOLF03	U85	82.7	Silty Sand	71.3	16.3	12.4	0.77	4.2
GOLW04	U100	100.0	Clayey Sand	71.5	14.2	14.3	0.64	4.5
OC0904	CSB66	66	Silty Mix	20.2	44.2	35.6	0.8	5.9
OC0904	CSB84	84	Silty Mix	33.2	36.7	30.1	0.77	5.4
OC0904	CSB92	92	Sandy Mix	39.7	35.9	24.4	0.65	5
OC0904	CSB100	100	Sand	78.3	12.2	9.5	0.93	4
OC0904	CSB112	112	Clayey Sand	69	13.5	17.5	0.88	5.1
OC0904	CSB123	122	Sand	76.7	8.6	14.7	Sand	6
OC0904	CSD58	58	Clayey Silt	17.8	48.3	33.9	1.6	7.61
OC0904	CSD84	84	Silty Mix	25	41.7	33.3	1.2	5.2
OC0904	CSD91	91	Silty Sand	72	15.9	12	0.72	4.8
OC0904	CSD100	100	Sandy Mix	45.2	29.1	25.7	1.2	5.4
OC0904	CSD107	107	Sand	75.6	11	13.4	0.72	4.2
EN0205	CSE55	59	Silty Mix	21.2	46.3	32.6	1.3	6.6
EN0205	CSE60	73	Silty Mix	21.8	46	32.2	1.2	6.4
EN0205	CSE70	?	Sandy Mix	45.5	29.8	24.6	0.92	4.1
EN0405	CSF50	85	Silty Mix	22.9	43	34.1	1.2	6.4
EN0405	CSG50	92	Sandy Mix	49.4	26.1	24.6	0.71	5.5
EN0405	#20	124	Gravel	85.7	7.1	7.3	0.92	3.1
EN0405	NCC80	103	Gravel	86.8	6.3	6.8	Sand	3.9
EN0205	CST135	126	Sand	80.3	6.9	12.8	0.68	4.3
OC0904	CSO121	121	Clayey Sand	71.4	10.7	17.9	0.81	5.7
OC0904	CFM138	138	Clayey Sand	65.1	14.2	20.7	1.6	5.9
EN0405	#3	126	Gravel	87.5	5.4	7.1	Sand	n/a
EN0405	NCC70	95	Clayey Sand	59.2	19.2	21.6	No Data	No Data
EN0205	J01	129	Gravel	89.4	4.6	6	Sand	n/a
OC0904	CSO163	163	Sandy Mix	43	30.3	26.7	No Data	No Data
OC0904	CSO159B	159	Sand	89.8	3.6	6.6	Sand	n/a
OC0904	CSO183	183	Clayey Silt	18.9	44.5	36.6	No Data	No Data
OC0904	CSO149	149	Clayey Silt	16	47.9	36.1	No Data	No Data

*Samples with too much sand to determine accumulation rates are listed as "sand".

**Samples not run (in the interest of time) are listed as No Data.

research indicates that near-shore sands exist out to approximately 20-30 m water depth (Martin, 1981; Courp and Monaco, 1990; Got and Aloisi, 1990; Certain, 2005).

Where the shelf begins to narrow due to a coastal promontory (Cap Bear), the across-shelf extent of the mud is reduced as the coastline extends seaward. Core U85 is uncharacteristically coarse-grained for its water depth (silty-sand) and therefore marks the narrowest extent of the M.S.M.D. (Fig. 6). South of this line, the mud deposit again extends seaward to form a crescent-shape parallel to the coastline. This deposit tapers out eastward, giving way to sands and gravels near the headland point.

In general, grain size tends to coarsen southward on the shelf. The finest sample collected was a silty-clay taken at site XX80 (the most northern core transect), while the coarsest samples were composed of sand and gravel taken at sites near Cap de Creus (cores J01, #3, and NCC80, Fig. 6). The R-line (south of Cap Bear) is an exception to this generality. Although still classified as muddy samples, these cores (R55 and R87) have greater amounts of sand (>30%) than those taken at similar depths elsewhere on the shelf (<30%). There does not appear to be significant down-core variability in grain-size for most cores collected on the western shelf (Fig. 6, inset).

Accumulation rates on the shelf vary from 0 – 2.5 mm/yr with consistently higher rates being associated with the M.S.M.D. (Fig. 7). Cores collected along the R-line (R55 and R87) reveal uncharacteristically low rates at water depths consistent with the M.S.M.D, indicating an area of sediment bypassing and reduced deposition. This

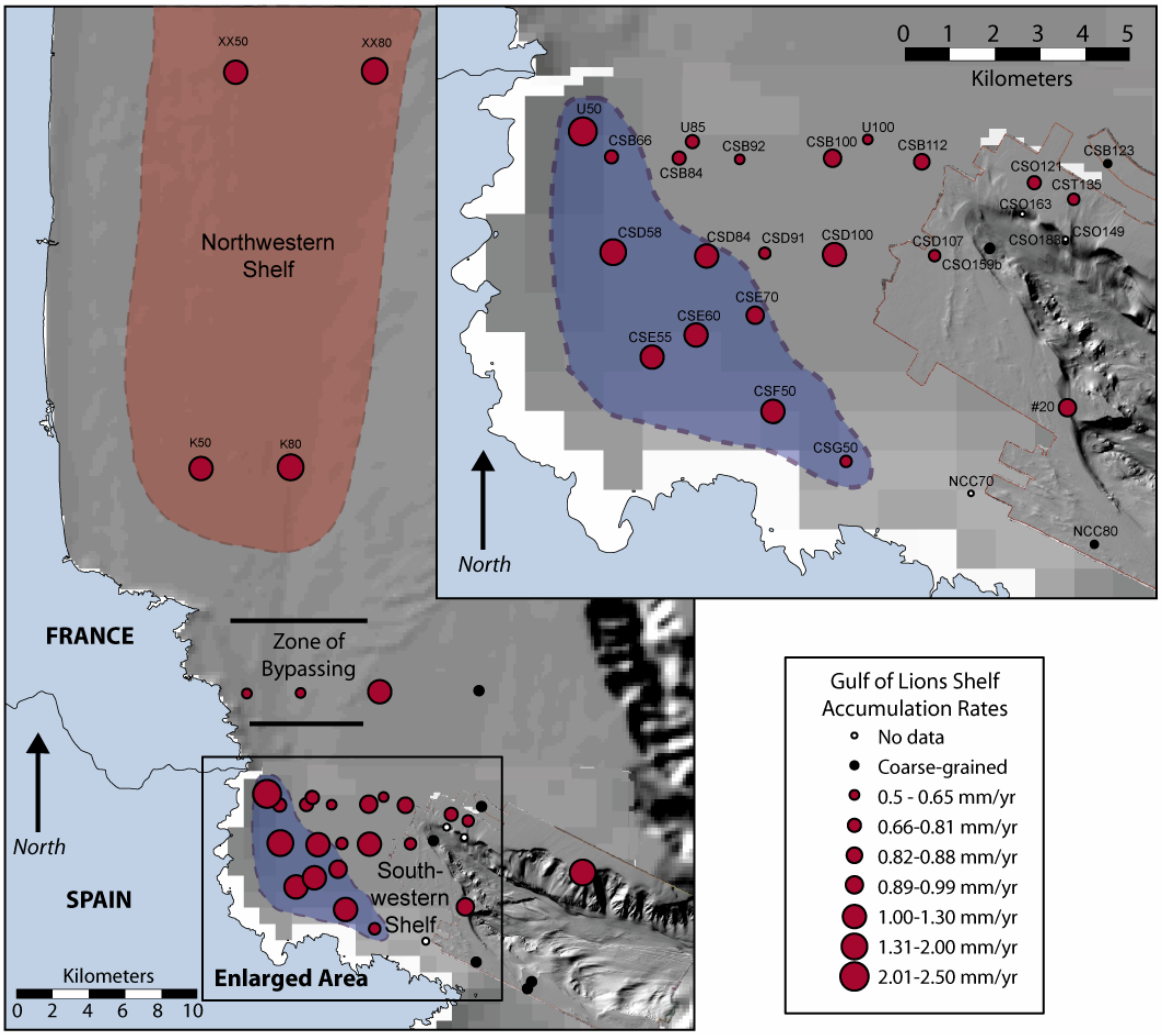

Figure 7. Shelf accumulation rates with depocenters and zone of bypassing. Northwestern shelf deposit is marked in red, the southwestern shelf deposit is marked in blue. The zone of bypassing represents an area of uncharacteristically low accumulation for that water depth. The enlarged view of southwestern shelf shows greater detail of the southwestern shelf sedimentation pattern.

area of bypassing suggests that there are two distinct "cells" of accumulation on the shelf: the northwestern-shelf M.S.M.D. (north of Cap Bear) and the southwestern shelf deposit (south of the Zone of Bypassing) (Fig. 7). Cores in the northwestern section tend to be finer-grained and have less variability than those in the southwestern section. Accumulation rates range from 1.0-2.0 mm/yr on the northwestern section of the shelf, with the highest rates occurring at 80-m of water depth. In the southwestern section, cores were generally sandier and the highest accumulation rate was 2.5 mm/yr at site U50. Accumulation rates on the southwestern shelf decrease southwestward, creating the crescent-shape deposit defined previously by grain-size characteristics. This deposit is in good agreement with a longer-time scale deposit identified in USGS Chirp seismic data on the lower portion of the shelf (M. Field and P. Hart, pers. comm.; Fig. 8).

4.1.2 Canyon Rim

Cores collected on the shelf at the canyon rim are sandy and tend to coarsen outward, creating deposits of >70% sand at locations adjacent to the canyon head (Fig. 6). Accumulation rates vary with location (Fig. 7). Comparison of core characteristics from the canyon rim to the north and south of Cap de Creus canyon reveals distinct differences. To the north, the shelf is predominantly clayey-sand (<70% sand with more clay than silt) with appreciable accumulation rates (i.e. 1.6 mm/yr at CFM138, Fig. 7). To the south, shelf cores are generally very coarse-grained (sand and gravel up to 4 cm at site J01) and show no evidence of fine-sediment accumulation (actual rates

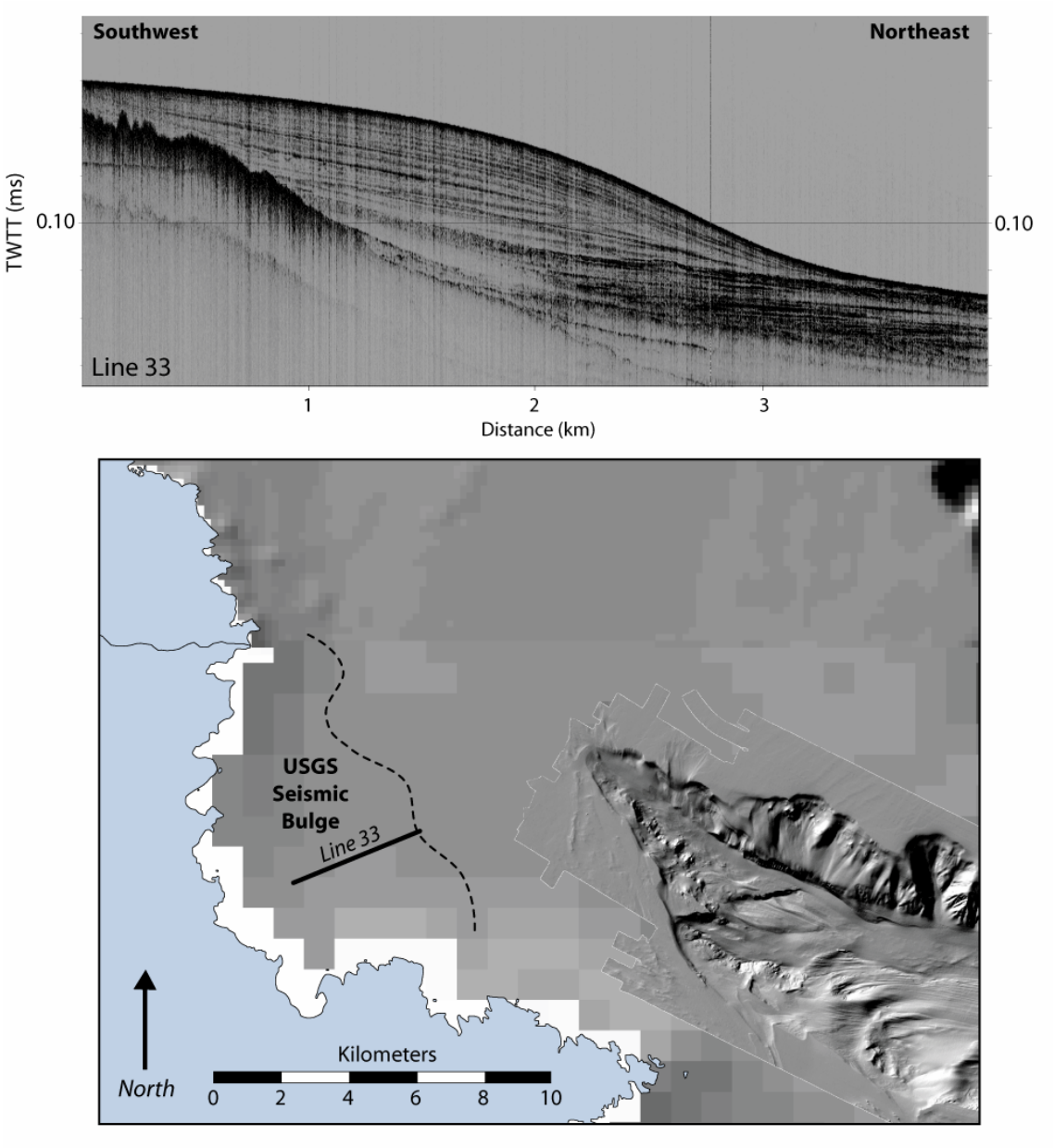

Figure 8. Seismic profile (line 33) and map of the southwestern shelf sediment bulge. Data courtesy of M. Field and P. Hart at USGS.

could not be determined due to the large proportion of coarse material in these samples) (Figs. 6 and 7). Box core attempts in this area returned only a few centimeters of coarse-grained and/or consolidated sediment despite high fall rates during core attempts. This indicates strong, resistive material not easily removed from its present setting (the southern rim of the canyon).

Sites that were reoccupied on different cruises showed little evidence of seasonal variation anywhere on the shelf. ^{7}Be was not detected in any of the cores collected on the Gulf of Lions western continental shelf.

4.2 Cap de Creus Canyon

4.2.1 Canyon Head and Thalweg

Surficial grain-size patterns and accumulation rates within Cap de Creus canyon are more complex than those on the shelf (Figs. 9 and 10, Tables 3 and 4). Surface sediments in the canyon head thalweg are coarse-grained (sand and shell hash) down to ~400 m water depth. The coarse-grained nature of these cores inhibit determination of accurate accumulation rates, but the sand layer in the canyon head was found to have above-supported levels ^{210}Pb activity, which indicates recent deposition (within the last 100 years). This surficial-sand layer unconformably overlies a stiff, consolidated gray mud with only supported levels of ^{210}Pb activity, indicating that the basal muds are older than 100 years (Fig. 11A). This distinct layering of coarse sediment overlying consolidated muds becomes less defined down-thalweg until it ceases at 300-400 m. At this point, there is a distinct switch to soft, unconsolidated muds

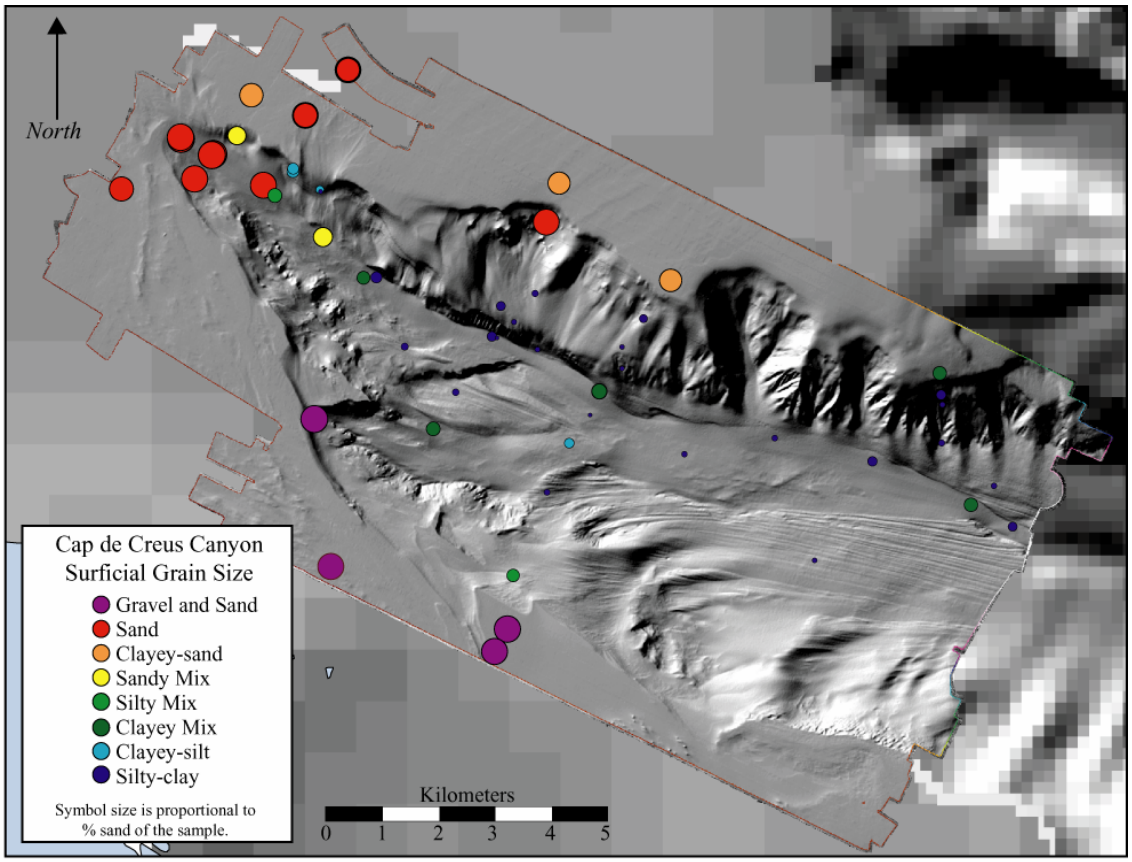

Figure 9. Surface grain-size distribution within Cap de Creus canyon. Colors represent sediment classification; symbol sizes represent % sand of each sample.

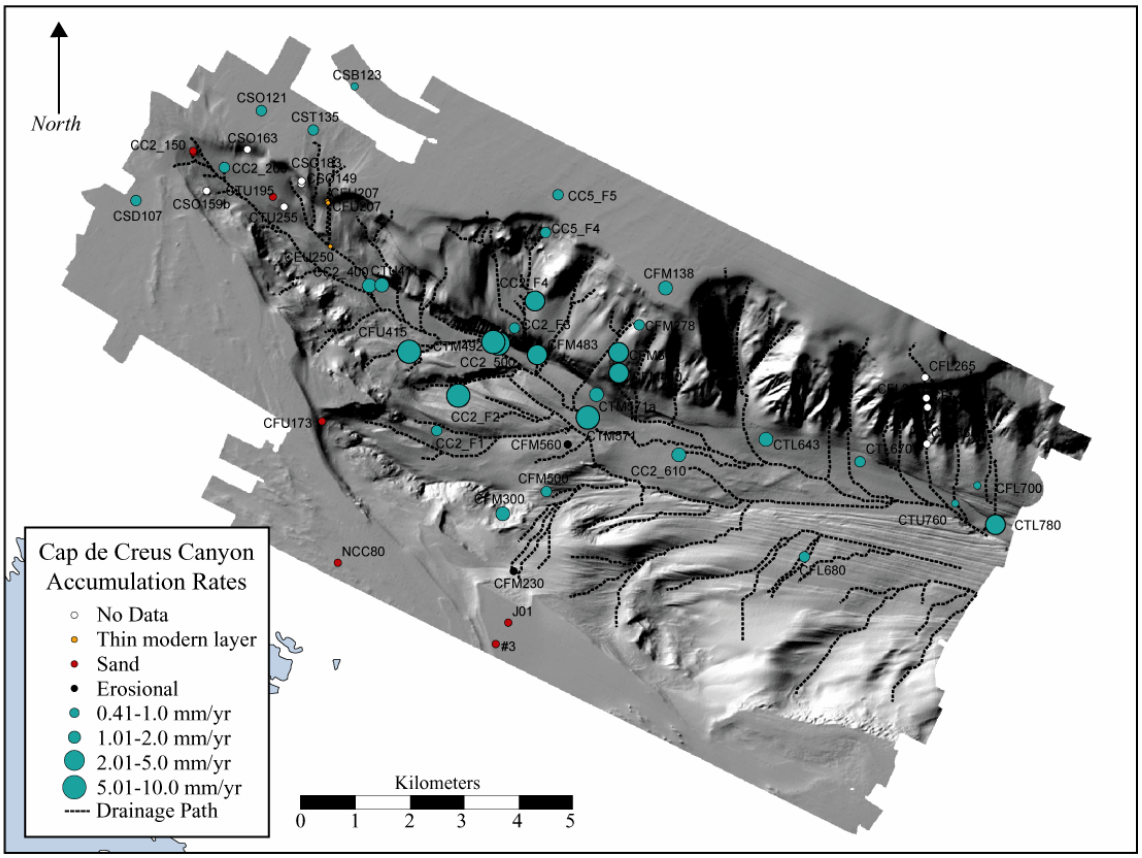

Figure 10. Canyon accumulation rates (based on ^{210}Pb data). Cores listed as "No Data" were not analyzed in the interest of time.

Table 3. Canyon thalweg core data

Cruise	*Core*	*Depth (m)*	*Grain Size*	*% sand*	*% silt*	*% clay*	*Accum. Rate (mm/yr)*	*Surface Activity (dpm/g)*	*Mud (cm)*
GOLF03	CC1_150	153	Sand	95	2.1	2.9	sand	2	
GOLW04	CC2_150	150	Sand	90.8	4	5.2	sand	3.2	
OC0904	CTU195	195	Sand	95.9	1.3	2.7	sand	1.9	
GOLF03	CC1_200	204	Sand	98.4	0.6	1	1	2.5	
OC0904	CTU231	231	Sand	87.8	4.9	7.4	sand	n/a	
OC0904	CTU255	244	Silty Mix	25.3	40.3	34.4	No Data	No Data	
GOLW04	CC2_400	407	Clayey Mix	22.1	33.3	44.6	1.7	11.3	4
OC0904	CTU411	411	Silty Clay	16.1	33.1	50.8	>1.6	11.1	5
EN0205	CTM492	501	Silty Clay	11.9	38.4	49.7	>6.7	14.9	9
GOLW04	CC2_500	512	Silty Clay	2	43.4	54.6	>7.7	15.3	12
OC0904	CTM571	571	Silty Clay	2	36.6	61.5	>5.8	19.5	13
EN0405	CTM571a	550	Clayey Mix	30.2	24.4	45.5	1.3	11.8	
GOLW04	CC2_610	614	Silty Clay	4.3	41.8	53.9	>2	18.2	8
OC0904	CTL643	643	Silty Clay	4.5	27.1	68.5	1.2	21.6	
OC0904	CTL670	670	Silty Clay	11.6	26	62.3	>0.8	20.6	3
OC0904	CTU760	760	Clayey Mix	23.7	27.7	48.7	No Data	No Data	n/a
OC0904	CTL780	780	Silty Clay	10.8	38.6	50.6	>3.5	20.6	4

*Samples with too much sand to determine accumulation rates are listed as "sand".

**Samples not run (in the interest of time) are listed as No Data.

***Samples with only a thin layer of modern sediment are listed as "layer".

****Samples marked with a " > " symbol are indicative of minimum values.

Table 4. Canyon flank core data.

Cruise	*Core*	*Depth (m)*	*Grain Size*	*% sand*	*% silt*	*% clay*	*Accum. Rate (mm/yr)*	*Surface Activity (dpm/g)*	*Mud (cm)*
OC0904	CFU173	173	Gravel	92.7	2.7	4.6	sand	2.2	
OC0904	CFM138	138	Clayey Sand	65.1	14.2	20.7	1.6	5.9	
OC0904	CFU207	207	Clayey Silt	8.7	40.8	50.6	layer	3.4	
EN0205	CFU207	213	Silty Clay	2.3	45.3	52.3	layer	1.6	
EN0205	CEU250	344	Sandy Mix	47.1	23.4	29.5	layer	7.4	
EN0405	CFM230	216	Silty Mix	20.3	42	37.7	erosiona;	n/a	
OC0904	CFM278	278	Silty Clay	8.4	33	58.5	0.7	17.6	
EN0405	CFM300	344	Silty Clay	10.8	35	54.2	1.3	13.5	
OC0904	CFM369	369	Silty Clay	2.8	36.5	60.7	3.2	17.8	
OC0904	CFU415	415	Silty Clay	6.6	36.7	56.7	>6.2	13.1	
OC0904	CFM440	440	Silty Clay	2.8	33.5	63.8	2.3	22.4	
OC0904	CFM483	483	Silty Clay	3.5	37	59.6	4.1	21.2	
EN0405	CFM500	483	Silty Clay	4.6	41.8	53.6	0.53	11.1	
EN0405	CFM560	565	Clayey Silt	12.6	44.6	42.8	erosional	1	
OC0904	CFL265	266	Clayey Mix	23.9	34	42.1	No data	No data	14
OC0904	CFL355	355	Silty Clay	12.5	35.9	51.6	No data	No data	
OC0904	CFL410	410	Silty Clay	4	44.8	51.2	No data	No data	
OC0904	CFL665b	665	Silty Clay	5.1	40.6	54.3	No data	No data	
OC0904	CFL680	680	Silty Clay	3.1	39.6	57.3	0.53	16.6	
OC0904	CFL700	700	Silty Clay	4.2	39.1	56.7	No data	No data	
GOLW04	CC2_F1	356	Clayey Mix	25.2	32.3	42.5	1	13.9	
GOLW04	CC2_F2	442	Silty Clay	5.9	43.2	50.9	>10	17.5	22
GOLW04	CC2_F3	386	Silty Clay	3.5	42	54.5	0.41	7.5	
GOLW04	CC2_F4	355	Silty Clay	5.5	34	60.5	2.7	17.8	
EN0405	CC5_F4	200	Sand	86.4	4.4	9.2	0.82	4.5	
EN0405	CC5_F5	131	Clayey Sand	63.7	14.7	21.6	0.95	5.4	

*Samples with too much sand to determine accumulation rates are listed as "sand".

**Samples not run (in the interest of time) are listed as No Data.

***Samples with only a thin layer of modern sediment are listed as "layer".

****Samples marked with a " > " symbol are indicative of minimum values.

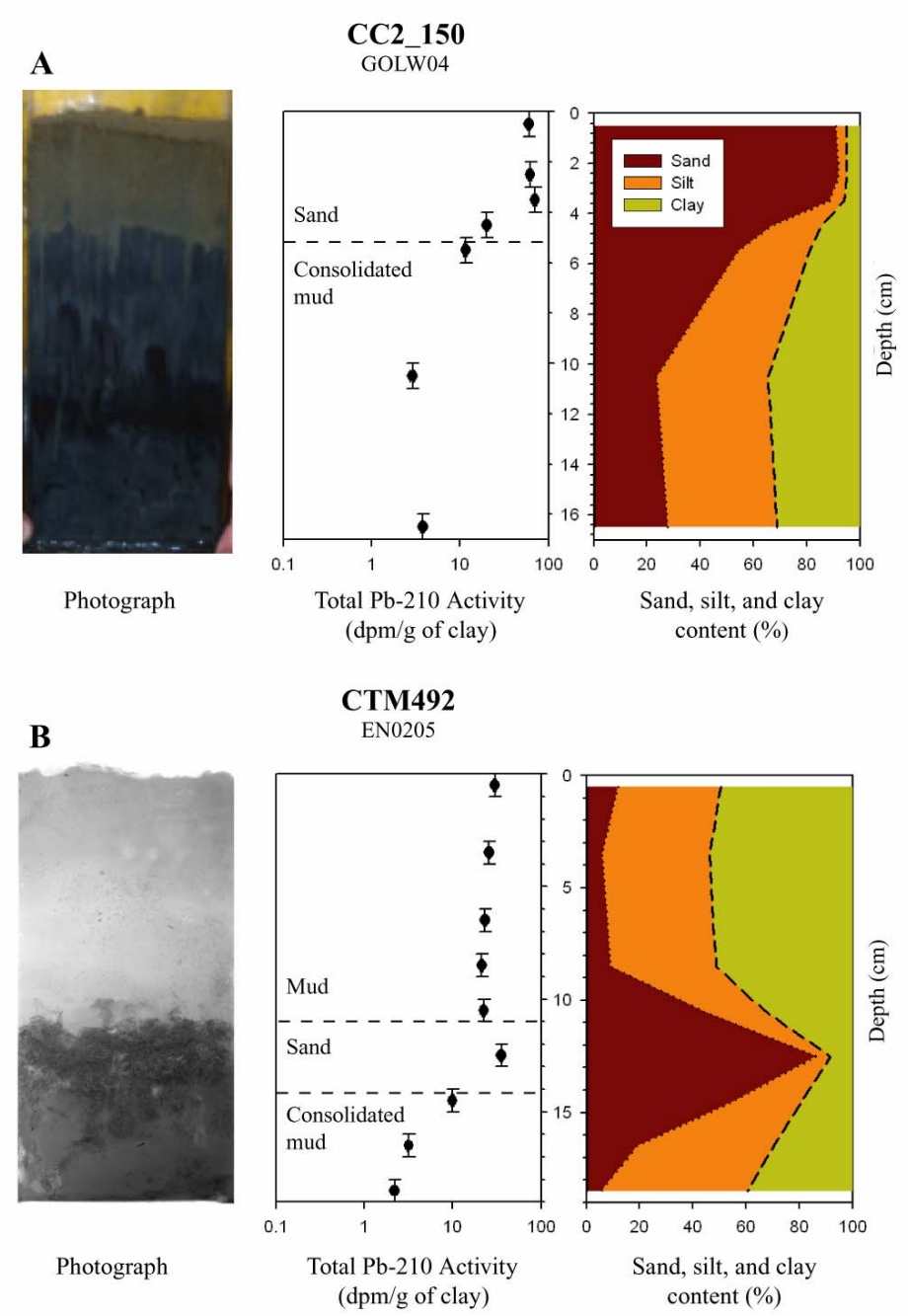

Figure 11. Sand layer and mud layer characteristics. (A) Core CC2_150, collected at 150 m water depth) shows a distinct activity changed between the upper sand layer and lower mud layer. The interim activities (4-6 cm) include some of the upper sands and some consolidated muds (due to angles of the erosive base). (B) CTM492, collected at 492 m water depth, reveals the recent mud layer and sand overlying consolidated mud. The interim activity at 15 cm is again attributed to mixing of sands with basal muds.

overlying coarser material in the thalweg region (Figs. 11B and 12). This pattern extends to the base of the study area. Within the thalweg, this mud layer is always underlain by coarse material (sand and shell-hash) (Fig 12).

The distinct mud-layer (varying from 4 – 22 cm in thickness) is primarily contained within the thalweg (Fig. 13). It is characterized by: (1) very fine grain-size (primarily silty-clays, coarsens slightly down canyon), (2) very low bulk density (average ~0.75 g/cm^3), (3) a lack of sedimentary structures, (4) relatively high surface $^{210}Pb_{xs}$ activities (> 25 dpm/g of clay) and (5) little or no evidence for down-core decrease of $^{210}Pb_{xs}$ activity within the layer (Fig. 13).

Minimum accumulation rates, determined by assuming that this layer had to be deposited within one half-life (based on the lack of down-core decrease in activity), suggests minimum accumulation rates between 5.0 and 10 mm/yr. Many of the thalweg coarse basal layers have above-supported levels of ^{210}Pb activity, indicating that they are also less than 100 years old. One thalweg core, CTM492, reveals consolidated mud unconformably underlying the sands seen elsewhere at the base of cores (Fig. 11). Cores collected on the near-thalweg southern flank are an exception to this generality: they are underlain by consolidated muds only and have no appreciable coarse-grained component (Fig. 13).

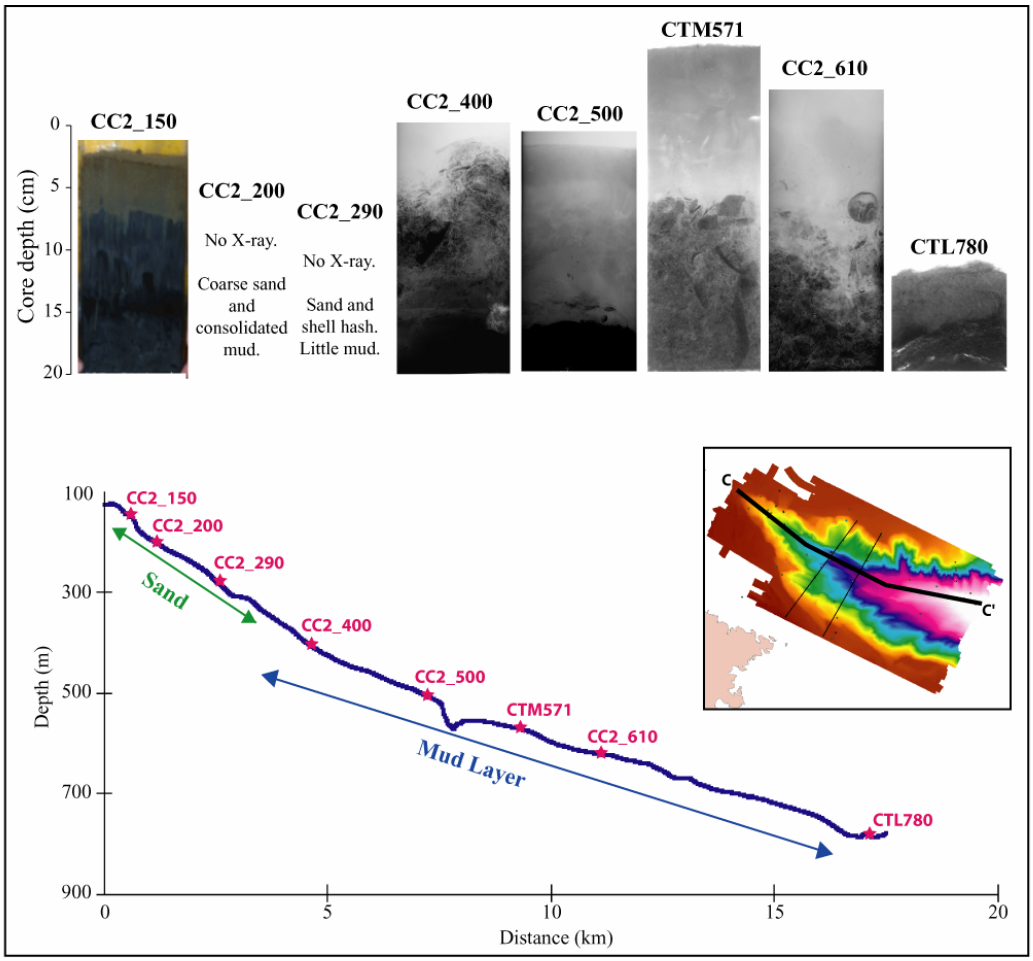

Figure 12. Down-thalweg profile of Cap de Creus canyon. Cores located from ~100 – 400 m water depth are generally coarse at the surface, while deeper there is a consistent mud layer overlying coarser material. Location of transect is shown in the depth diagram on the right.

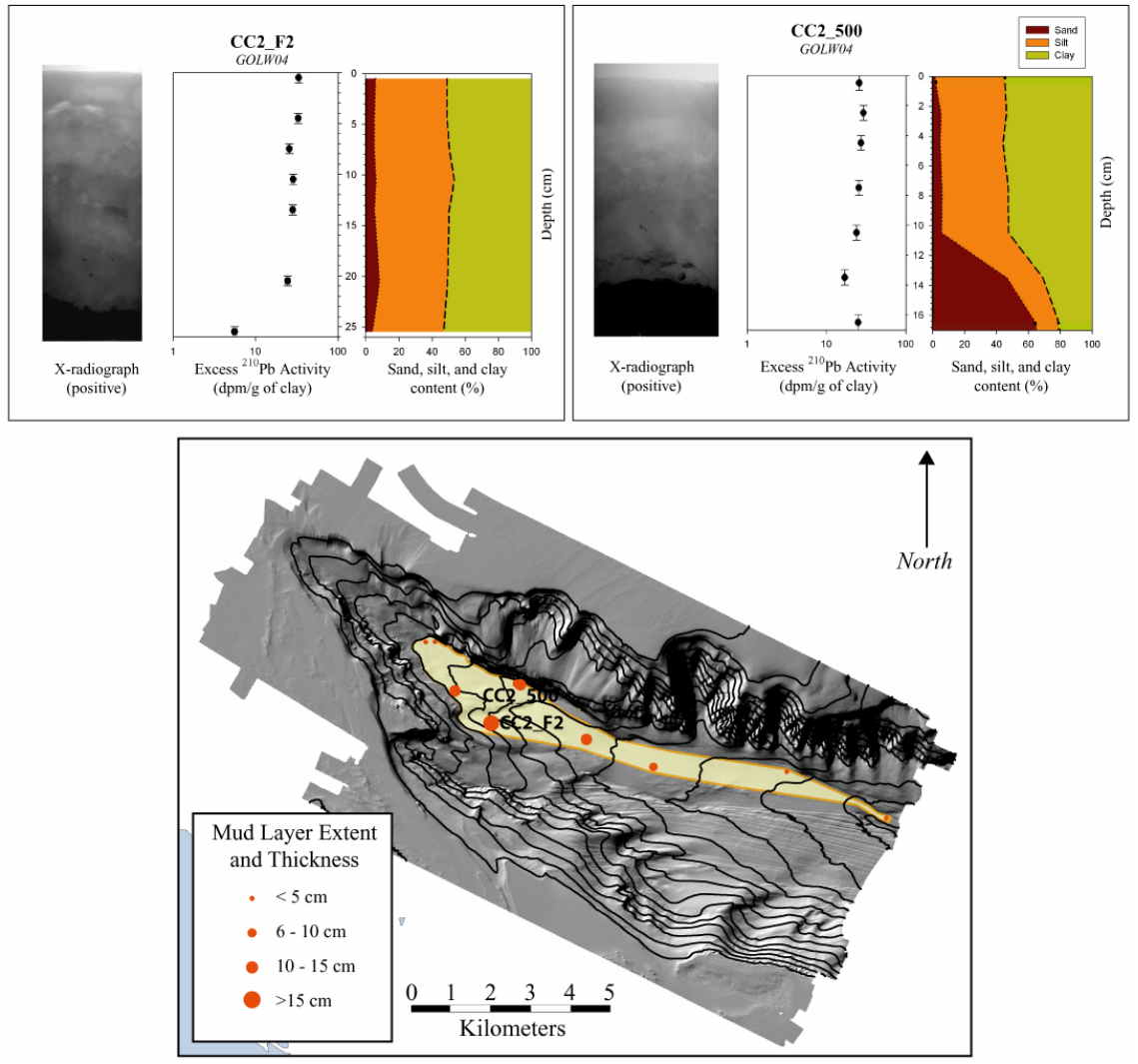

Figure 13. Mud layer extent and core characteristics. The mud layer extends from ~400 m in the thalweg to ~780 m (the limit of the study area). It reaches onto the near-thalweg southern flank, but is primarily confined to the thalweg. Examples of the mud layer are shown above. They reveal the lack of decrease of $^{210}Pb_{xs}$ activity with depth and change of grain-size (CC2_500) or consolidation (CC2_F2) with depth.

4.2.2 Northern and Southern Flanks

Accumulation rates on the flanks are quite variable, ranging from 0 mm/yr to greater than 4.1 mm/yr (Fig. 10). Two across-canyon profiles indicate asymmetry in accumulation rates on the canyon flanks, but it is less apparent at shallower depths than at deeper depths within the canyon. Transect A-A' shows a clear differentiation between the canyon flanks: significantly more accumulation occurs on the northern flank than the southern (Fig. 14). Most cores collected on the northern flank have accumulation rates greater than 1.5 mm/yr, while those on the southern side are either erosional (as evidenced by the presence of only consolidated muds) or have very low accumulation rates (e.g. 0.53 mm/yr, Fig. 14). The cores taken within the thalweg have high accumulation rates associated with the thalweg mud deposit discussed previously (e.g. core CTM571).

The cross-canyon profile B-B' (centered around core CC2_500), shows active accumulation on both flanks in this part of the canyon (Fig. 15). Whereas the highest accumulation rate is located on the near-thalweg southern flank (CC2_F2, >1.0 cm/yr), this area is within the broader thalweg and was likely affected by the same processes as the central channel of the thalweg (where the mud layer has also been observed, CC2_500). It is also important to note that no cores were collected on the upper, steep part of the southern flank. This profile shows less asymmetry between flanks than is evident in transect A-A'.

High-resolution multi-beam bathymetry of Cap de Creus canyon reveals evidence of furrows on the southern flank (Fig. 16). The one core taken within the

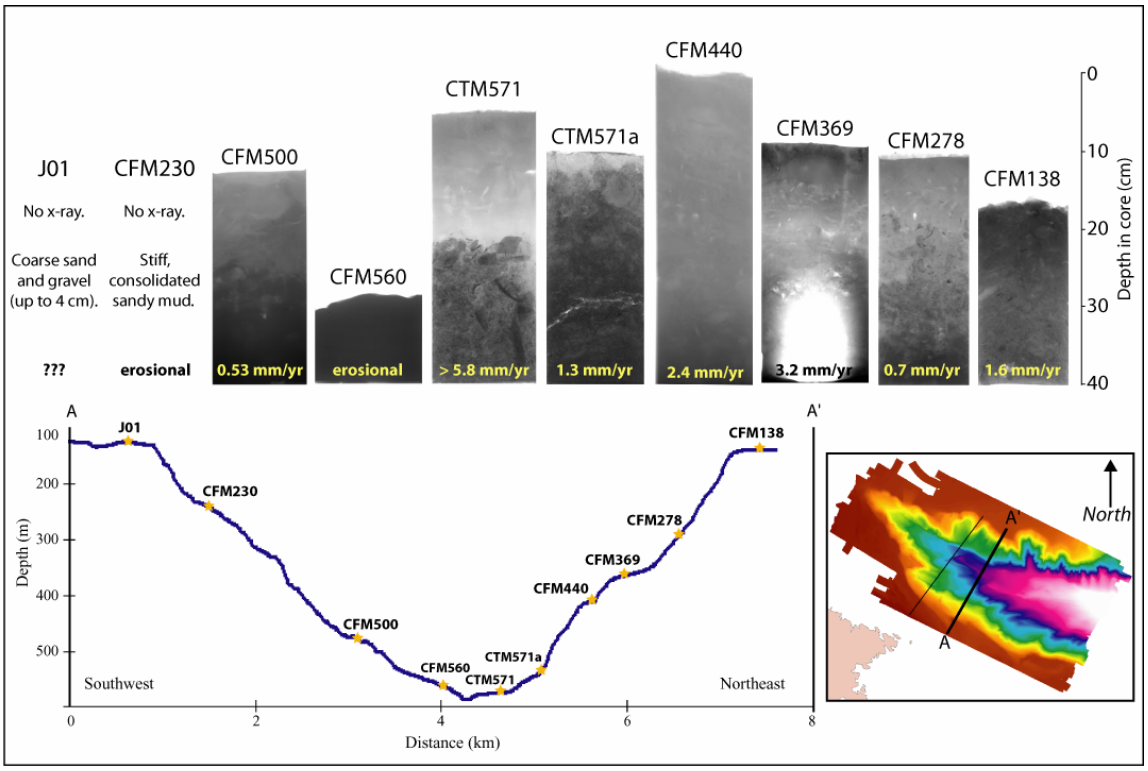

Figure 14. Lower (A-A') cross-canyon profile. The profile shows extreme asymmetry within the canyon: cores collected on the northern flank all show relatively high accumulation rates (excluding CFM278, which is on a very steep slope), while those taken from the southern flank are coarse-grained, erosional, or have low accumulation rates.

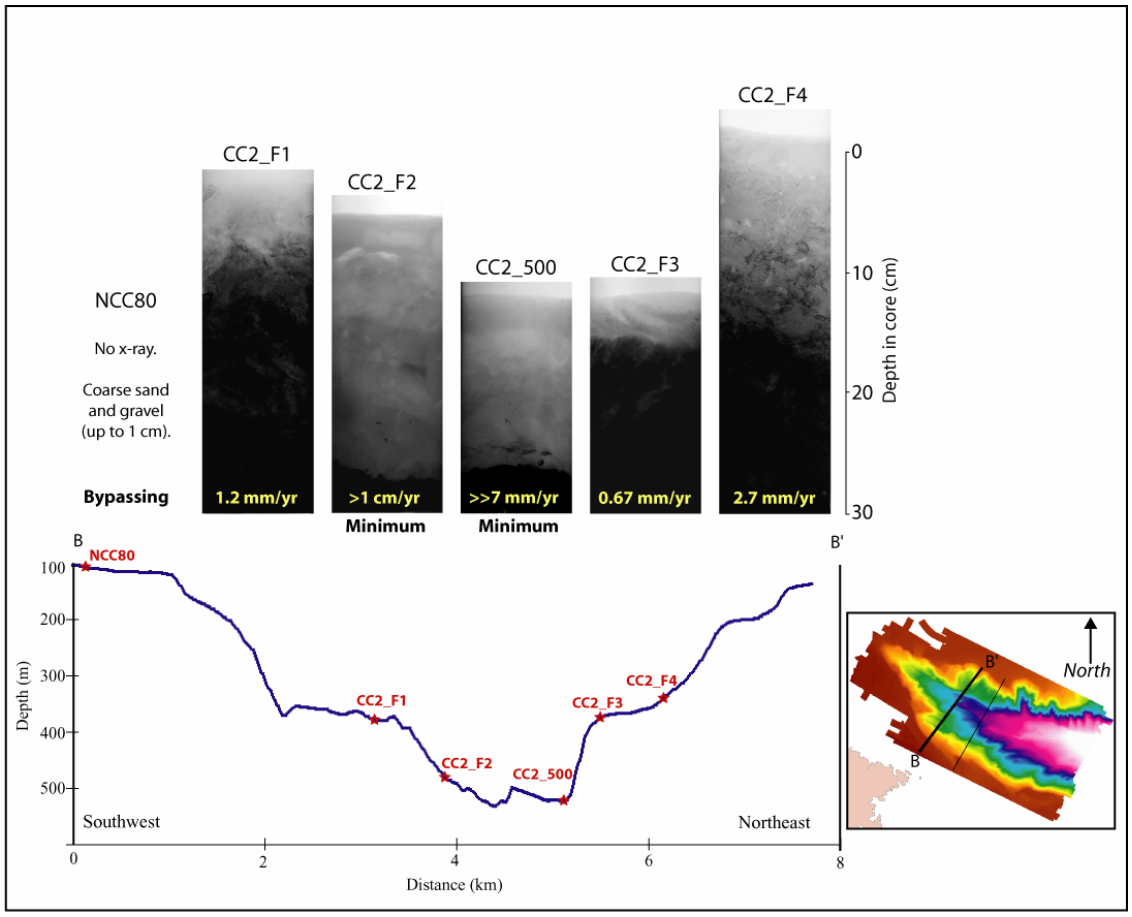

Figure 15. Upper (B-B') cross-canyon profile. The profile shows significantly less asymmetry across the canyon (accumulation on the southern flank), although no cores were collected on the upper portion of the southern flank. Core CC2_F2 looks similar to thalweg cores in the mud-layer, suggesting that this region is affected by similar fine-grained processes as the thalweg.

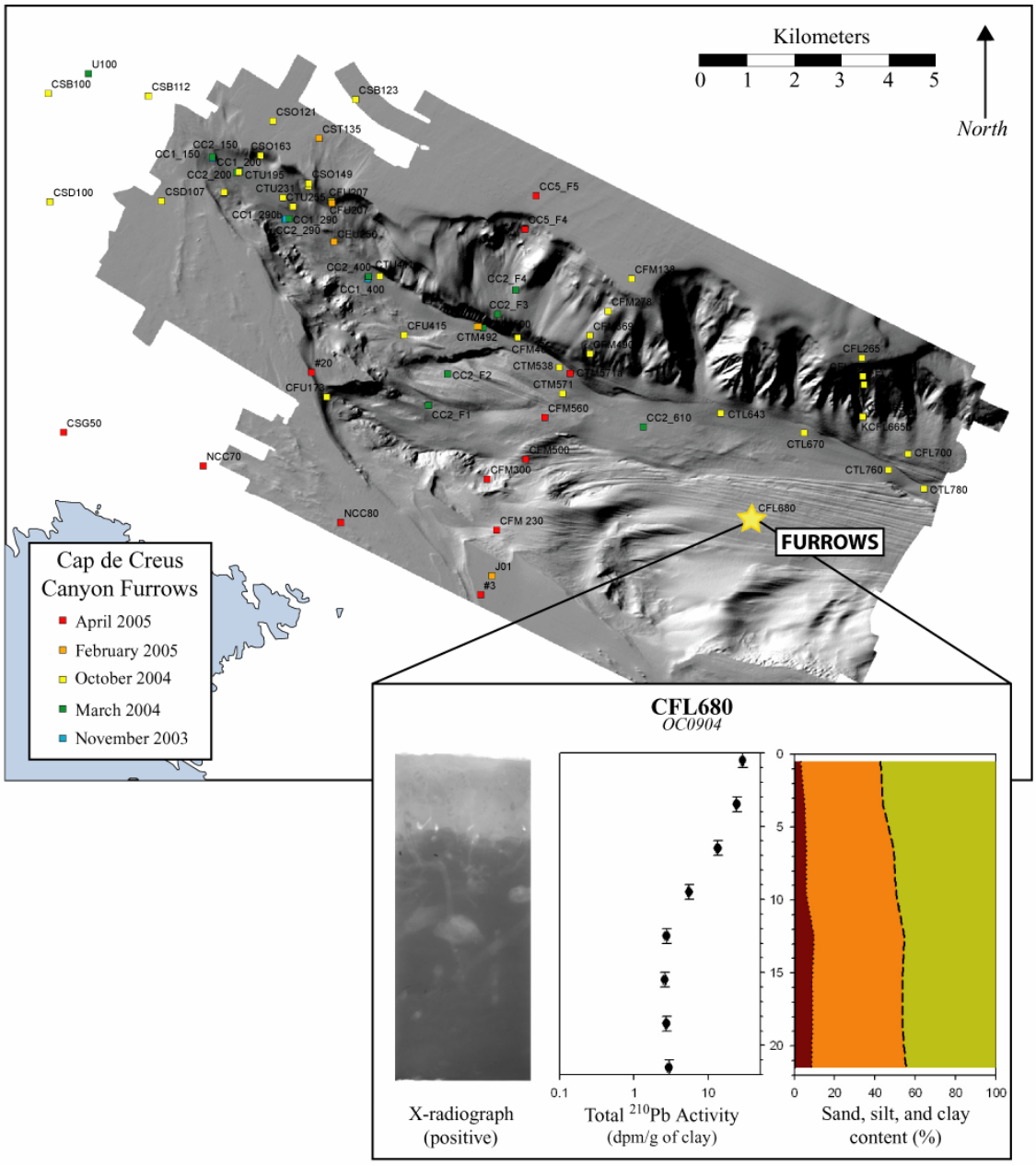

Figure 16. Canyon furrows location and characteristics. Furrows are visible over much of the southern flank of Cap de Creus canyon. Core CFL680, collected from the furrow field, has a low accumulation rate (0.53 mm/yr), although sampling techniques limit the ability to define this core as characteristics of the crest or gully.

furrows (CFL680) is composed primarily of silty-clay that accumulated at a rate of 0.53 mm/yr. Due to limitations of ship-board sampling, there is no way to know if the core sampled sediments on the furrow or trough.

Reoccupation of sites within the canyon showed little evidence of seasonal variation. Within the thalweg mud layer, thicknesses varied slightly but spatial resolution was too low to know if this was simply an artifact of sampling variability. No mud-layer cores were reoccupied in April 2005; as a result, any changes to the mud layer in this time period would not have been observed by this study. Similar to the shelf, ^{7}Be was not detected in any of the canyon-core samples.

4.3 Ancillary Data

Interpretations of these results were greatly enhanced by collaboration with other scientists: Acoustic Doppler Current Profiles (ADCP, supplied by X. Durrieu de Madron) show acceleration of surface currents near Cap Bear, at the northern edge of the coastal promontory (Fig. 17). These data also show current deviations to the west on the southwestern portion of the shelf, which may be indicative of eddy formation over the southwestern shelf. Although this is only a snap-shot of variable currents (collected in November 2003), it does suggest a general pattern of currents around the headland.

Current data derived from a tripod and three moorings within the canyon were supplied by P. Puig and A. Palanques (Fig. 18). These data show currents moving primarily up- and down-thalweg at 145-m water depth (1 meter above bottom), while at 200-m and 500-m water depth (both taken at 5 mab), there is an additional southward-

flow component. At the deepest site (750-m), the southward-component disappears and is replaced by a northeastward flow that reaches maximum speeds greater than 80 cm/s. All instruments at all depths within the canyon record some up- and down- thalweg currents. Records of temperature, current speed, and suspended sediment concentration at these instruments sites (also supplied by P. Puig) show a distinct correlation between decreased temperature, increased current speeds, and heightened suspended sediment concentration (as determined by transmissometer data), particularly at the deepest mooring site (Fig. 19).

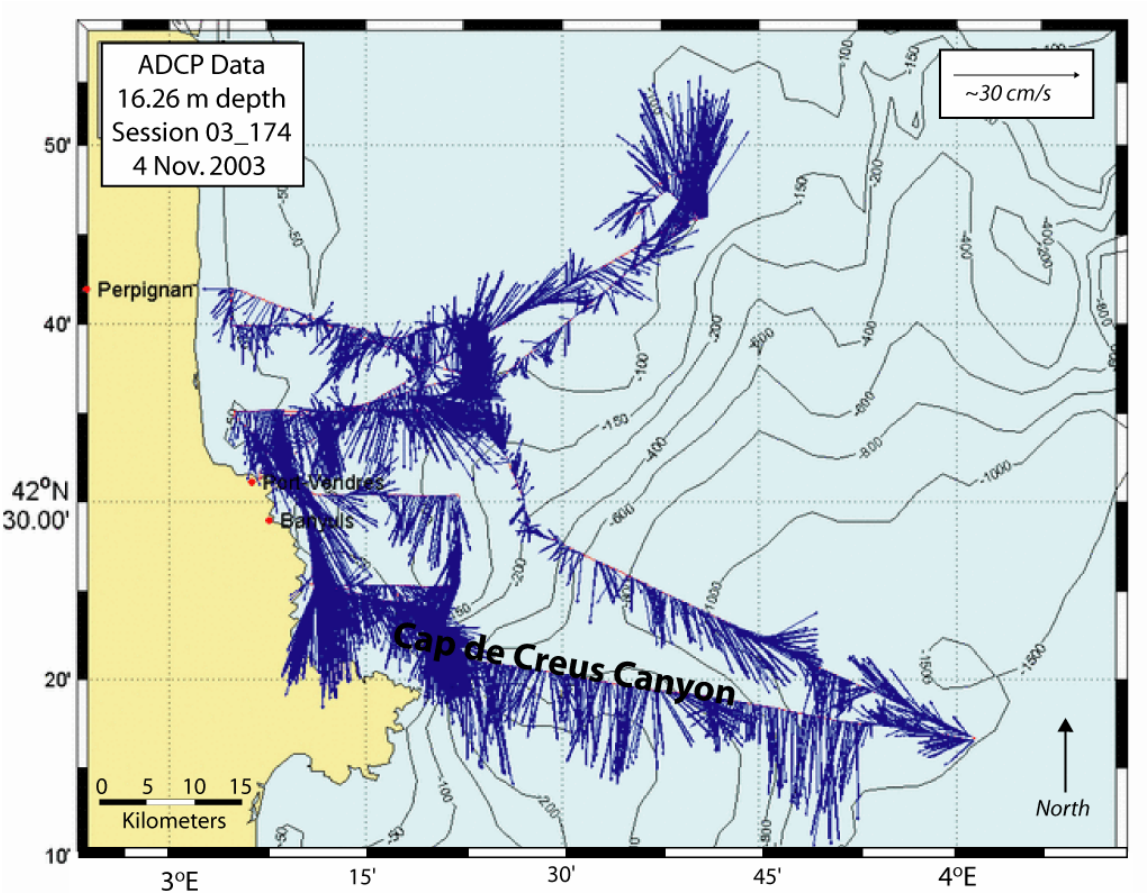

Figure 17. ADCP data from the western Gulf of Lions. Data collected in November 2003 shows current acceleration around the coastal protrusion and possible impedence effects associated with Cap Bear and Cap de Creus headlands. Maximum speeds are approximately 30-35 cm/s. (Data courtesy of X. Durrieu de Madron, CNRS-INSU.)

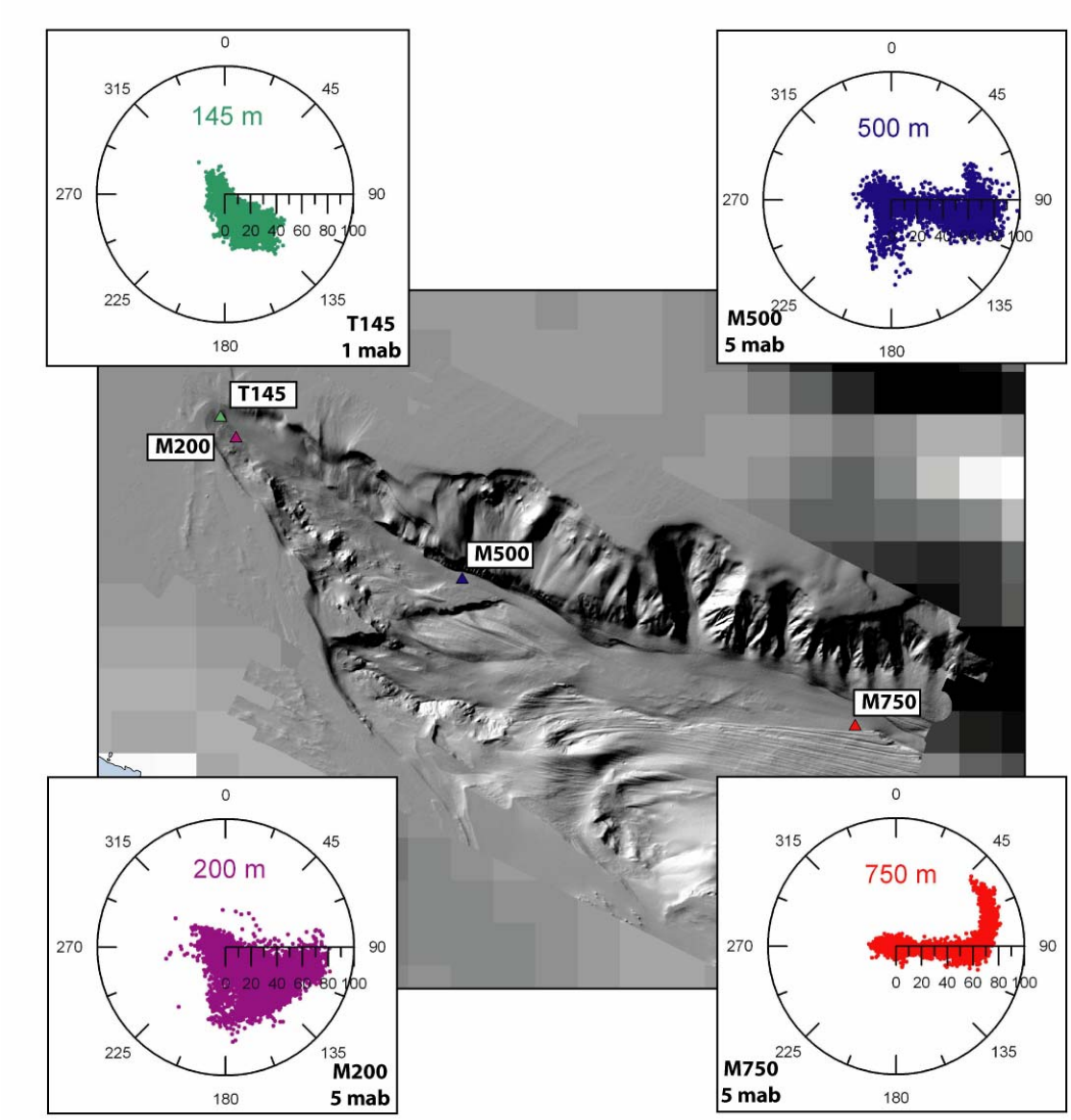

Figure 18. Current patterns within Cap de Creus canyon. Polar plots of time-series data indicate current speed and direction. Radial numbers represent current direction (0 is to the north). Speeds are in cm/s. T145 measurements, recorded by a tripod in the canyon head) were taken at 1 meter above bottom (mab), while the remainder were recorded by moorings at 5 mab. In general, at 150 m water depth, currents generally run parallel to the canyon axis. Deeper in the canyon (200 and 500m), a southward component is visible with the along-axis flows. At the deepest site, the southward flows are replaced by flows towards the northeast, suggesting a different hydrographic regime at this location. (Data courtesy of P. Puig.)

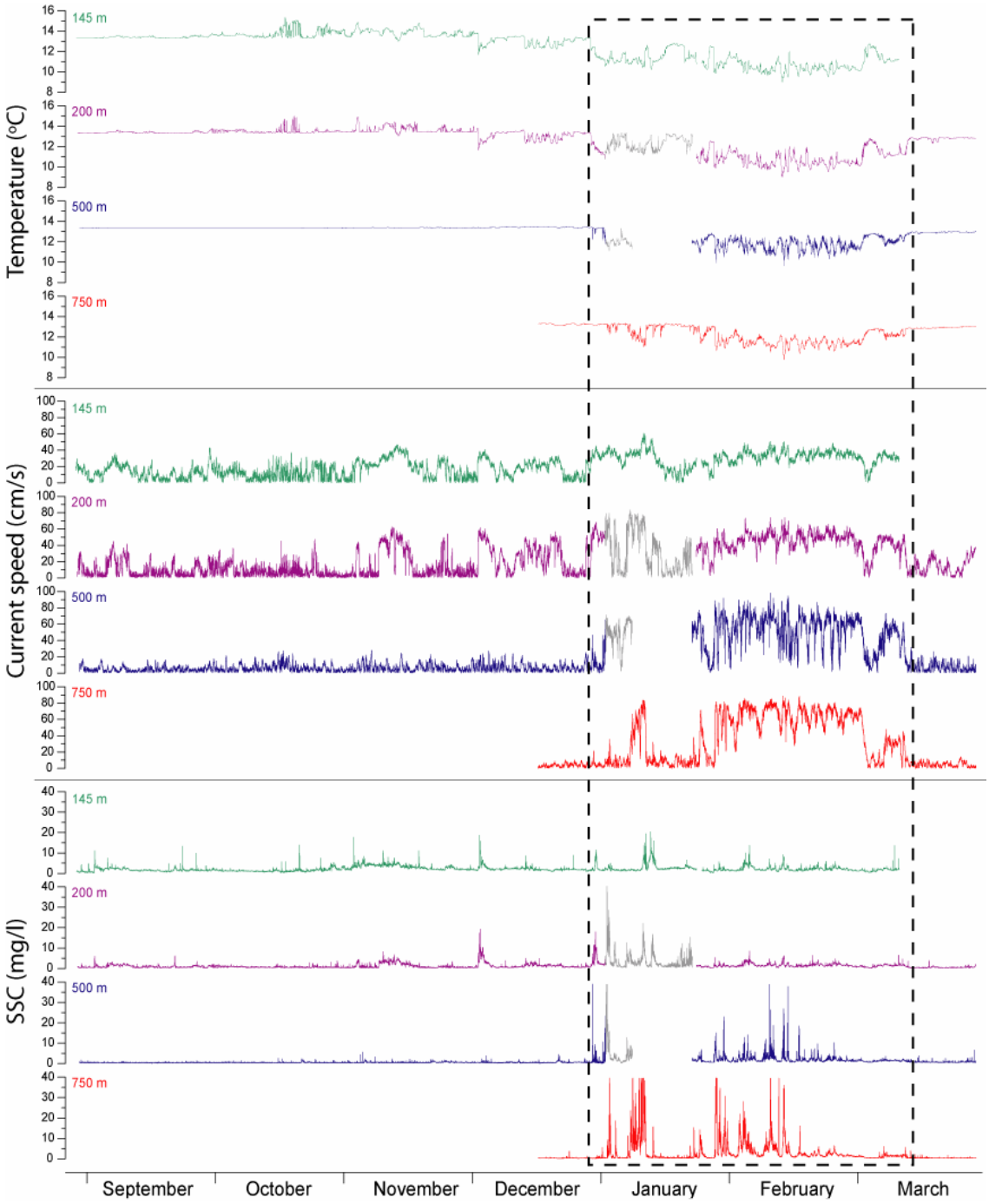

Figure 19. Current flow characteristics within Cap de Creus canyon. Line color represents location within the canyon (green = 145 m, purple = 200 m, blue = 500, and red = 750 m). Instrument data shows a strong correlation between cold temperatures, fast currents, and high-suspended sediment concentrations (SSC) during the winter months. (Data courtesy of P. Puig.)

5. DISCUSSION

5.1 Shelf Sedimentation Processes

5.1.1 Across-shelf Accumulation Patterns

Grain-size patterns and accumulation rates on the shelf indicate that fine-grains are primarily accumulating at mid-shelf depths (30-85m), which is in agreement with previous studies (Martin, 1981; Got and Aloisi, 1990, Certain, 2005) (Fig. 7). Many margins around the world have similar across-shelf patterns, with enhanced accumulation beginning at the inner shelf-midshelf boundary and greatest rates occurring in the midshelf region (Nittrouer and Wright, 1994). These mud deposits are commonly underlain by a transgressive sand layer, which can be reworked in the nearshore environment (where wave energy is high) and exposed on the outer shelf (where sediment supply is trapped or limited). This pattern of mid-shelf deposition is recognized on shelves worldwide (regardless of sediment supply) due to changes in the ability of surface waves to impact the seafloor under increasing water-depths (Nittrouer and Sternberg, 1981; Nittrouer and Wright, 1994). Similar patterns of enhanced mid-shelf deposition are observed on the Washington continental shelf and the Amazon shelf, as well as other locations within the Mediterranean (Nittrouer and Sternberg, 1981; Got and Aloisi, 1990; Nittrouer and Wright, 1994).

Got and Aloisi (1990) describe a model for across-shelf sediment transport in the Gulf of Lions within which the benthic nepheloid layer (BNL) is primarily responsible for fine-sediment deposition on the shelf. In the near-shore environment, waves frequently generate sufficient energy to rework sands and keep fine-sediments in

suspension (Got and Aloisi, 1990). This BNL can then move across the shelf via hydrographic forcing (e.g. downwelling) or gravity-driven flows (Nittrouer and Wright, 1994). Once the BNL enters water-depths below wave-base (where waves no longer affect the bottom), fine particles begin to settle out and create the mid-shelf mud deposit. Upon reaching the outer shelf, particles remaining in suspension in the BNL are too small to be deposited if affected by current velocities as low as 10 cm s^{-1}, thereby causing them to move southwestward with the general flow and leave the outer shelf bare of modern sediment deposits (Got and Aloisi, 1990).

A decrease in grain-size from 50 to 80 m water-depth on the shelf (as is visible in XX-line, Fig. 6) supports this model. At shallower depths (where there is more potential wave-energy), coarser sediments are deposited (e.g. clayey-silt at XX50) but finer sediments are held in suspension and do not settle out until deeper depths (eg. Silty-clays at XX80).

5.1.2 Along-shelf Accumulation Patterns

Active sediment accumulation south of all major fluvial sources in the Gulf of Lions indicates that there is a southward trend of sediment movement along the shelf (Fig. 8). The primary forcing mechanism for this transport is a general southward flow that moves along the entire shelf (P. Puig, pers. comm.). This southward flow, which can be enhanced by meanders of the LPC current onto the shelf, causes sediment contained in shelf BNLs (see section 5.1.1) to be transported long distances to the south before accumulating on the bed.

However, smaller-scale variations in flow regulate specific deposit characteristics (i.e. faster flows tend to leave coarser grains) (Boggs, 2001). Such variations in flow can be created by current interactions with headlands, which have long been known to exert controlling influences on coastal currents and flows (Davies et al., 1995; Pawlak and MacCready, 2002). Headlands become a prominent feature within the southwestern portion of the Gulf of Lions and likely dominate along-shelf variations in sedimentary deposits. The two shelf deposits (northwestern and southwestern) and the dividing zone of bypassing are subject to different hydrographic regimes which can be explained by these current interactions. ADCP data, collected by X. Durrieu de Madron, shows a snapshot of the different currents possible within each section (Fig. 17).

Northwestern shelf – This region has a smooth coastline and experiences a general southward flow throughout the year, which suggests little flow disturbance in this zone (P. Puig, pers. comm.) These coastline conditions are similar to other parts of the gulf, which suggests that this area is affected by similar sedimentation processes (and produces similar depositional patterns) as the eastern gulf (i.e. an epicontinental prism, Got and Aloisi (1990), Courp and Monaco (1990), and Certain et al (2005)).

Zone of Bypassing – Near Cap Bear, the seabed is sandier than to the north (36% sand at R55 relative to less than 20% sand at K50) (Fig. 6). This coarser grain-size, combined with lower accumulation rates (<1.0 mm yr^{-1}) in this portion of the shelf, are indicative of inhibited deposition due to current acceleration in this area (Boggs, 2001). ADCP data recorded near Cap Bear in November 2003 capture significantly strong surface currents moving towards the southeast, suggesting current acceleration around

the headland (X. Durrieu de Madron, pers. comm., Fig. 17). This acceleration is hypothesized to be caused by the Venturi effect, which dictates that when a confined flow encounters a restriction, it must speed up to compensate for reduced pressure created by the formation of a pressure gradient behind the restriction (X. Durrieu de Madron, pers. comm.). In the western Gulf of Lions, the flow restrictions are Cap Bear and Cap de Creus. The offshore flow boundary (which is required for the Venturi effect to be valid) is likely the LPC current on the outer shelf. Analogous current acceleration around a headland has been documented by Geyer and Signell (1990) and Geyer (1993). The variability of these strong flows around Cap Bear and Cap de Creus is unknown. However, the geographic correlation between the seabed data and current information suggest that this acceleration around the headland likely controls the reduced deposition of fine sediments.

Southwestern shelf – Accumulation rates increase in the southwestern portion of the shelf, reaching 2.5 mm/yr at site U50 (Fig. 7). Less sand (relative to the bypassing region) is present in this sample as well (e.g. R55, <25%) (Table 2). These factors suggest that the currents preventing deposition in the Zone of Bypassing are not affecting the southwestern shelf. Rather, enhanced deposition in this region suggests that flow separation (associated with current deflection around Cap Bear) may increase deposition in this area. Geyer (1993) has documented the creation of eddies on the down-flow side of coastal headlands on a smaller scale, while Davies et al. (1995) have also shown eddy formation at the lee side of a cape (assuming flows were sufficiently fast) at larger scales using modeling. This type of eddy has been shown (using modeling)

to erode fine sediments and move sands in shallow-water (<20 m), suggesting that they can have significant impacts on the seabed (Signell and Harris, 2000). In deeper water, the strength of the eddy on the bottom would likely be reduced, allowing deposition as opposed to erosion. The conceptual model presented here is that as coastal currents are deflected by Cap Bear, part of the flow moves off the shelf around Cap de Creus, while another part circulates as an eddy on the southwestern shelf. Eddies are hypothesized to cause enhanced accumulation below their center, suggesting this mechanism as a probable cause for enhanced sediment deposition on the southwestern shelf.

5.1.3 Longer-term Accumulation Patterns

Comparison of modern data (from this study) with longer-timescale seismic data obtained by the USGS shows the same general pattern of accumulation on the shelf: a bulge developing on the southern portion (Fig. 8). Seismic Chirp data were not collected on the northwestern portion of the shelf in this study, so comparisons cannot be made. However, the correlation between core data and seismic studies suggests that little has changed over time on the shelf and modern processes are representative of processes that have been occurring over longer-timescales.

5.1.4 Canyon Rim Accumulation Patterns

Accumulation rates and grain-size distributions on the northern and southern rim are drastically different (Figs. 7 and 8). Northern rim cores were composed of fine sand with a significant mud fraction (35% mud) (Table 2). Accumulation rates were

appreciable (1.6 mm/yr at CFM138, 0.95 mm/yr at CC5_F5), indicating that sediment is reaching this area (Fig. 10). The southern rim is composed of very coarse material (gravel up to 4 cm at J01) and consolidated material (see section 4.1.2), which is indicative of fast currents scouring the shelf and preventing fine sediment deposition.

This comparison suggests that the rim to the north of the canyon is an area of some deposition and therefore represents a potential sediment pathway to the upper canyon, while the southern rim is an area of sediment bypassing that may provide an entryway to the deeper parts of the canyon. Energetic currents that allow little or no sediment to be deposited in the upper canyon appear to control the seabed characteristics on the southern canyon rim (P. Puig, pers. comm.).

5.2 Canyon Sedimentation Processes

Within Cap de Creus canyon, each section (outlined in Fig. 5) is classified as depositional or non-depositional with respect to fine grains:

- Northern flank: High accumulation rates (up to 4.1 mm/yr) and fine-grain sizes (primarily silty-clays) indicate an area of fine-sediment deposition over a 100-year timescale (Fig. 10).
- Mid-depth thalweg: The presence of the mud layer with little ^{210}Pb activity decrease with depth indicates rapid sediment accumulation in this region (4-22 cm in less than 22 years) (Fig. 13). The near-thalweg southern flank is included in this section due to its similar characteristics to those cores collected within the thalweg proper.

- Canyon head: The recent sands contain little to no fine sediment (generally >90% sand). Therefore, this region is classified as non-depositional for modern muds. It is, however, likely an area of coarse-grained transport and deposition.
- Southern flank: Erosional features (i.e. CFM560), low accumulation rates (0.53 mm/yr at CFM500), and the presence of gravel (J01) suggest that this is an area of bypassing. As such, it is classified as non-depositional for fine-grains on the 100-year timescale.

5.2.1 Fine-grained Sediment Sources to the Canyon

Enhanced deposition of fine-grains on the northern flank (relative to the southern) suggests that fine-sediments are entering Cap de Creus canyon from the northern rim (Fig. 14). The significant asymmetry of accumulation rates within the canyon (high rates on the northern flank, lower rates or erosion on the southern), as well as modern sediment accumulation on the rim adjacent to the northern flank (1.6 mm/yr at site CFM138), provides evidence of this preferential deposition, as well as a source for it. It is hypothesized that currents transport the shelf benthic nepheloid layer (BNL) over the canyon rim, where a portion of it detaches to form an intermediate nepheloid layer (INL). This INL can then move across the canyon, supplying sediment to the northern (and southern) flank.

The strongest evidence for this conceptual model is mooring data collected within the canyon. Current meters at 200 m and 500 m (both 5 mab) in the canyon show

a distinct southward flow (maximum speed of ~50 cm/s) within the canyon (Fig. 18). These southward flows have appreciable suspended sediment concentrations (generally ~ 5 mg/l), indicating that they are probable sources of sediment to the canyon (P. Puig, pers. comm.) (Fig. 19).

This proposed mechanism also is supported by transect B-B', which documents some deposition on the near-thalweg southern flank of the canyon (Fig. 15). Deposition by nepheloid-layer advection is the most probable way to get deposition on both flanks in the narrow region of the upper canyon. These intermediate nepheloid layers (created by detachment of shelf BNLs) can be advected across the entire width of the upper canyon and extend distances past the main axis and onto the opposite flank, allowing deposition on both sides of the canyon (Baker and Hickey, 1986).

The fine-grain sizes collected on the northern flank (primarily silty-clays, see Table 3) also suggest deposition by particle settling through the water column. These detached BNLs produce INLs over the canyon, from which sediment is deposited on the flank. Got and Aloisi (1990) report the presence of a defined BNL (very low concentrations, ~ 1 mg/l) extending to the shelf-break, which indicates that these bottom layers are present in the Gulf of Lions. Similar to Quinault canyon (Washington coast), it is hypothesized that as the regional currents move over the canyon, the increase in depth and deflection of the isobars cause them to slow, allowing enhanced deposition relative to the shelf (Carson et al., 1986; Hickey et al., 1986).

Within the Gulf of Lions, nepheloid-layer advection of sediment into a canyon has been observed in Lacaze-Duthiers canyon (located directly to the northeast of Cap de

Creus canyon) and Grand-Rhone canyon (Durrieu de Madron, 1990; Durrieu de Madron, 1999; Frignani, 2002) (Fig. 1). Advection of nepheloid layers off the adjoining shelf is also seen on other margins, such as Quinault canyon on the Washington coast (Hickey et al., 1986; Baker and Hickey, 1986; Carson et al., 1986; Snyder and Carson, 1986). The direction of sediment movement into the canyon varies seasonally and by margin, but the process of intermediate nepheloid-layer advection facilitating deposition in canyons is a well-documented characteristics of margin sedimentation.

5.2.2 Fine-grained Sediment Bypassing

If advective transport of nepheloid layers were the only process occurring within Cap de Creus canyon, one would expect deposition across the entire southern flank. However, while there are some small pockets of accumulation on the southern flank (Fig. 15), sediments were generally consolidated or coarse-grained material devoid of modern sediment. This type of deposit is generally representative of a high-energy environment not reflective of hemipelagic sedimentation from nepheloid layers. Therefore, environmental conditions must be fundamentally different on the southern flank, which (1) prohibits sediment deposition in this part of the canyon, or (2) removes the sediment after it is deposited.

Data collected within the canyon at 750 m water depth (and to a lesser degree at the 500 m site) show currents that flow due east (along the thalweg) with frequent and significant currents (up to 80 cm/s) directed towards the northeast (Fig. 18). These are counter to the southward-flowing across-canyon currents observed at shallower depth in

the canyon. The alignment of this flow corresponds well geographically with the gravel-laden, southern-rim shelf cores (which also indicate fast current movement), suggesting that the same flows may be scouring the southern rim and flank.

Mooring data from within the canyon suggest that these currents are created by the cascading of dense-water off the Gulf of Lions continental shelf. These flows record a distinct correlation (particularly at the 750-m mooring site) between fast currents (up to 80 cm/s) and decreased temperature (ranging from ~10-12° C, relative to the 13.2° C in the ambient Levantine intermediate water), which is consistent with characteristics of dense-water (Durrieu de Madron, 2005) (Fig. 19). Further, the most intense flows occurred from December to February, a time of known dense-water formation on the Gulf of Lions continental shelf (P. Puig, pers. comm.)

Previous hydrographic studies have identified the western Gulf as a primary location of annual dense-water formation and cascading off the shelf (Millot, 1990; Durrieu de Madron et al., 2005*).* Recent work has suggested that after formation, much of this dense water is pushed southward along the shelf by Tramontane winds and the general current regime within the Gulf (P. Puig, pers. comm.). Once it encounters Cap de Creus headland, the flow is impeded and the dense-water begins to pool on the outer southwestern shelf until it spills into Cap de Creus canyon from the southern rim (P. Puig and X. Durrieu de Madron, pers. comm.). These near-bottom gravity flows inhibit sediment deposition and erode sediments that may have been deposited on the southern flank (P. Puig, pers. comm.). This conceptual model is consistent with the erosional seabed observed on the southern rim (Fig. 6).

The moorings also recorded a strong correlation between dense-water flows and high suspended sediment concentrations (up to 40 mg l^{-1}), suggesting that these flows are able to move large amounts of sediment into and through the upper canyon (Fig. 19). However, since the flow speeds and concentrations are still great at 750-m water depth (near the base of this study), sediments must be carried past the upper canyon and deposited deeper in the canyon, seaward of the present study area (P. Puig, pers. comm.). These dense-water flows appear to be a second mechanism supplying sediment to Cap de Creus canyon, although it is not deposited in the study area. Large amounts of sediment are moving off the shelf and through the upper canyon, making Cap de Creus canyon a important conduit of sediment export from the Gulf of Lions continental shelf.

5.2.3 Canyon Thalweg Processes – Coarse Grains

While nepheloid-layer advection and dense-water cascading are able to explain the preferential deposition on the northern flank, they are not effective at explaining the sand in the canyon head. The above-supported levels of ^{210}Pb activity, which can extend to the base of the sand layer (~6 cm at CC2_150), suggest that the sand has been emplaced recently (within the last 100 years) (Fig. 11). This pattern of modern sands continues down to at least 600 m water depth within the canyon thalweg and includes those sands which are situated below the thalweg mud layer (Figs. 11 and 13). Sands at greater depth (>600m) have much lower excess ^{210}Pb activities; these sands cannot be definitively classified as modern because of the potential mixing of sand grains with the overlying modern mud during subsampling.

This suggests that modern sands are not extending past ~600 m water depth in the thalweg. It is worthwhile to note that while modern, these sands need not have been released onto the margin recently. Rather, they may be relict sands which have been transported, which allows them to acquire a modern ^{210}Pb signal while interacting with the water column. The classification of modern sand in this paper means only that this has recently moved into the canyon, but says nothing about its emplacement on the shelf.

Based on the prominence of sand in the head and its general confinement within the thalweg, the canyon head is the most probable site of entry for these coarse grains (Fig. 9). The mechanism that moves these sediments to the canyon head, however, is less clear. Movement of coarse-material at great depths (~100 m at the shelf break) requires high-energy transport, such as a gravity-driven flow (e.g. turbidity current) within the submarine canyon. There are four scenarios that have been put forth to explain sand transport into submarine canyons:

- Slope erosion and failures – Slope erosion and failure is a possible option for moving coarse-grains into a canyon. Oversteepening of sands near the canyon head would cause gravity-driven flows to move down the thalweg. It is not clear what would induce these failures in Cap de Creus canyon, but they are known to be effective in the headward erosion of submarine canyons.
- Wave-orbital liquifaction of sediment in the canyon head – Puig et al (2004) documented generation of gravity-driven flows within Eel canyon (California margin) due to liquefaction of sediments caused by increasing pore pressures resulting from wave oscillations at the shelf break. For this method to effectively

generate gravity-flows, the inputed sediment must have some degree of interparticle cohesive bonds and low permeability to allow an increase in pore pressure (Puig et al., 2004). This is an unlikely possibility for the coarser sands found in the canyon head, which have little cohesion and are quite permeable, making them less susceptible to changes in pore-pressure.

- Interception of littoral and/or outer-shelf sand transport – Canyons off the coast of California have been shown to intercept littoral transport of sands, allowing direct transport of coarse material from the nearshore environment to deep-sea fans (Paull et al., 2003; Paull et al., 2005). Scripps canyon (which is not directly connected to a river), also shows patterns of sand supply to the canyon head by nearshore littoral drift (Fukushima et al., 1985). This is an unlikely mechanism for Cap de Creus canyon because the canyon is separated from the nearshore littoral transport zone (<20 m water depth) by the M.S.M.D. However, if there were a mechanism moving sands along the outer shelf (similar to nearshore littoral transport), Cap de Creus could behave similarly to California canyons, which penetrate much closer to shore. A possible mechanism of sand-movement on the outer-shelf has not been identified by this study.
- Up- and down-canyon flows – Along-axis flows were recorded by instruments as shallow as the head of Cap de Creus canyon (Fig. 18). These flows have been observed in many canyons (i.e. Quinault and Grand-Rhone) as a result of current interaction with isobaths (Baker and Hickey, 1986; Durrieu de Madron, 1994). In Cap de Creus canyon, the flows recorded in the head averaged ~30 cm/s at 1

mab, with maximum speeds of ~60 cm/s (Fig. 19). Using empirical data reported by Miller, McCave, and Komar (1997), it is estimated that currents of 30 cm/s and 60 cm/s at 1 mab would move grains of ~80 μm and 0.9 mm (9000 μm), respectively. Considering these estimates, it is possible that these along-axis flows are moving sands within the canyon head when they reach maximum values. However, the presence of the mud layer deeper in the canyon suggests that these currents are not consistently effective through the entire canyon and rather must be focused within the head. The mechanism of this focusing is unknown.

Unfortunately, the dominant mechanism causing sand transport and deposition within Cap de Creus canyon can not be determined with the present data set. Regardless of the mechanism however, the presence of these modern sands suggests sand input at the canyon head.

5.2.4 Canyon Thalweg Processes – Fine Grains

The mud layer that overlies the thalweg sands from ~400 – 780 m water depth is indicative of rapid, non-steady state deposition within the canyon (Fig. 13). One of the most distinguishing characteristics of this layer is the minimal amount of isotopic decay with depth in the core. If this deposit had accumulated slowly over time (even over one half-life), the activity at the base of the layer should be only half of the surface activity (Fig. 20). Rather, there is a distinct break between relatively constant excess-activity levels and the underlying supported levels (Fig. 13). This suggests that these are not

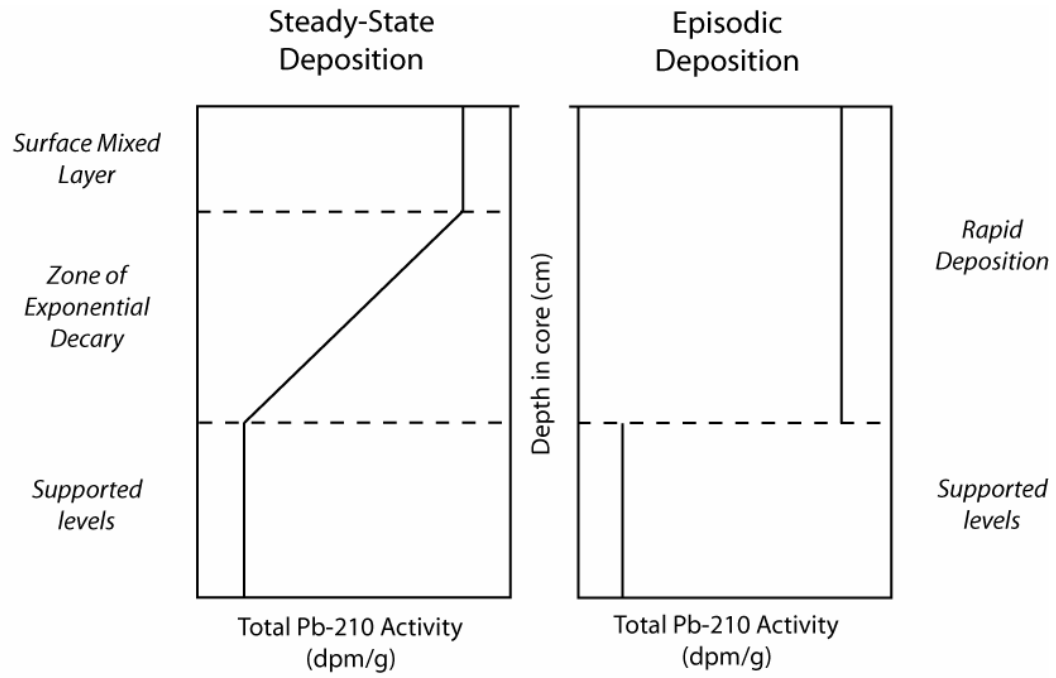

Figure 20. Theoretical ^{210}Pb profiles for different depositional mechanisms. The steady state profile (left side of diagram) shows consistent decreases in activity with depth from the surface mixed layer to supported levels. The episodic deposition (right side) shows a distinct shift at a specific depth plane, indicating a break in deposition followed by rapid accumulation (no decrease in activity with depth).

steady-state deposits; rather, they were deposited very rapidly (Mullenbach, 2002). A conservative estimate for accumulation rates can be calculated assuming the entire deposit was laid-down in less than one half-life (steadily over 22 years). This estimate gives accumulation rates up to 1.0 cm yr^{-1} for the mud layer. However, the actual short-term deposition rate is likely much higher because deposits are formed episodically (annual to decadal timescales). The low bulk-density throughout the layer is further suggestive of rapid deposition of this mud layer.

The lack of sedimentary structure within this mud-layer opens the possibility that these mud deposits have accumulated under steady-state conditions, but are so biologically-mixed that they appear to be episodic layers. If the initial $^{210}Pb_{xs}$ activity of sediment reaching the seabed is consistent across the canyon, then an estimate of the excess activity of a biologically-homogenized sediment layer can be calculated using steady-state profiles from the northern flanks. The assumption is that the thalweg deposits could have looked similar to the northern flank cores prior to homogenization (e.g. steady-state deposition). This calculation shows that $^{210}Pb_{xs}$ activities would be lower (10 – 18 dpm/g of clay) throughout the homogenized layer (if biological mixing were to produce the constant activity with depth.) than is actually found in the thalweg mud layer (~25 dpm/g of clay). This suggests that this mud layer is likely not the result of biological mixing of steady-state deposits.

The source of this mud is not clear, but there are two possibilities: deposition by down-thalweg gravity-driven flows or advection of nepheloid layers. Preferential accumulation within a thalweg (relative to canyon flanks) has been also observed in

Quinault canyon (Washington coast), a canyon dominated by hemipelagic deposition (Thorbjarnarson et al., 1986). However, the mechanism causing focusing of sediment in topographic lows (although previously documented) is not fully understood (Carson et al., 1986). Data from the northern flank of Cap de Creus canyon shows that hemipelagic sedimentation is dominant in that area, similar to Quinault canyon; this suggests that similar focusing mechanism may be operating in the thalweg, which would enhance deposition and create the mud-layer.

The abrupt shift to supported ^{210}Pb activities at depth (CTM492, Fig. 11) indicates that the mud layer is periodically flushed out (i.e. there is a loss of stratigraphic time in the sediment column). Probable mechanisms are (1) dense-water cascading through the thalweg that erodes the mud layer or (2) gravity-driven sediment flows down the main thalweg. The former could erode sediment that had been deposited over short timescales, moving the sediment deeper into the canyon (P. Puig, pers. comm.). The latter could remove previous deposits and leave new, upward-fining deposits consistent with a turbidity current (Boggs, 2001). The second theory has two major flaws: a lack of gradational, upward-fining in the cores (grain-size transitions tend to be sharp), and the lack of an sufficient source of fine-grains near the shelf break that could be incorporated into the gravity flow. This suggests that dense-water cascading is the more probable option for flushing sediment from within Cap de Creus upper canyon. Regardless of the supply and flushing mechanisms of this mud layer, the rapid deposition and removal is good evidence that significant amounts of material are moving through Cap de Creus canyon over short (annual to decadal) timescales.

5.3 Sediment Delivery to the Western Gulf of Lions

^{7}Be was not detected in any of the cores collected on the shelf or canyon. This suggests that the sediment deposited in the western portion of the Gulf has been in the system (i.e. removed from its fluvial source) for at least 3-4 months. This is not unexpected, considering the distance between the western region and the Rhone (~160 km), which is the primary sediment source. However, it is also possible that there is no fluvial source of ^{7}Be in this area. Rivers where sediments are stored in alluvial plains or not efficiently moved through the drainage basin may release sediment with no initial ^{7}Be (Sommerfield et al., 1999).

5.4 Sediment Budgets

In order to determine the relative importance of this region in sequestering sediments, a semi-quantitative budget was created for the western Gulf of Lions shelf and Cap de Creus upper canyon. The annual amount of sediment deposited was calculated based on the following equation:

$$M_t = \sum (A_i)(M_i \cdot \rho_i)$$

Where M_t is the total sediment mass for a defined section, A_i is the surface area for the section, ρ_i is the average bulk-density (based on modern sediments), and M_i is the sediment thickness for that area, which is defined as:

$$M_i = (R_i) \cdot (1\ \text{yr})$$

where R_i is the ^{210}Pb-derived accumulation rate. For calculations involving the thalweg mud-layer, the thickness used was the average of the mud-layer thicknesses in all cores

collected in that section. On areas without complex bathymetry (such as the continental shelf), the accumulation rates and bulk densities will likely be similar over spatially-large scales. However, within the canyon, where there are dramatic bathymetric changes over smaller scales, there may be significant variability at the canyon scale. M_t is defined for each physiographic zone (Fig. 5), using mean accumulation rates and bulk densities for each area individually. A rough estimate of the total amount of sediment accumulating within Cap de Creus upper canyon and on the western Gulf of Lions continental shelf is then calculated by summing the mass of all areas.

Areas are defined based on the depocenters previously identified in this study. All calculations are based on fine-grained sediment only. On the shelf, boundaries are set as the extent of the M.S.M.D. (approximately 30-85 m water depth) and the Zone of Bypassing (Fig. 21). Within the canyon, the four main areas used in calculations are similar to those defined previously: the canyon head, the mud-layer (in the thalweg), the northern flank, and the southern flank (Fig. 22). The mud-layer is further divided into 3 sections: M1-M3, which were distinguished by the mud-layer thickness within each section.

Budget calculations for the shelf reveal that $(53 \pm 5.6) \times 10^4$ metric tons of sediment are accumulating each year on the northwestern shelf and $(4.0 \pm 1.0) \times 10^4$ tons accumulate yearly on the southwestern shelf (Fig. 21, Table 5). In total, this amounts to $(57 \pm 5.7) \times 10^4$ tons of sediment that accumulate each year in this portion of the Gulf of Lions shelf.

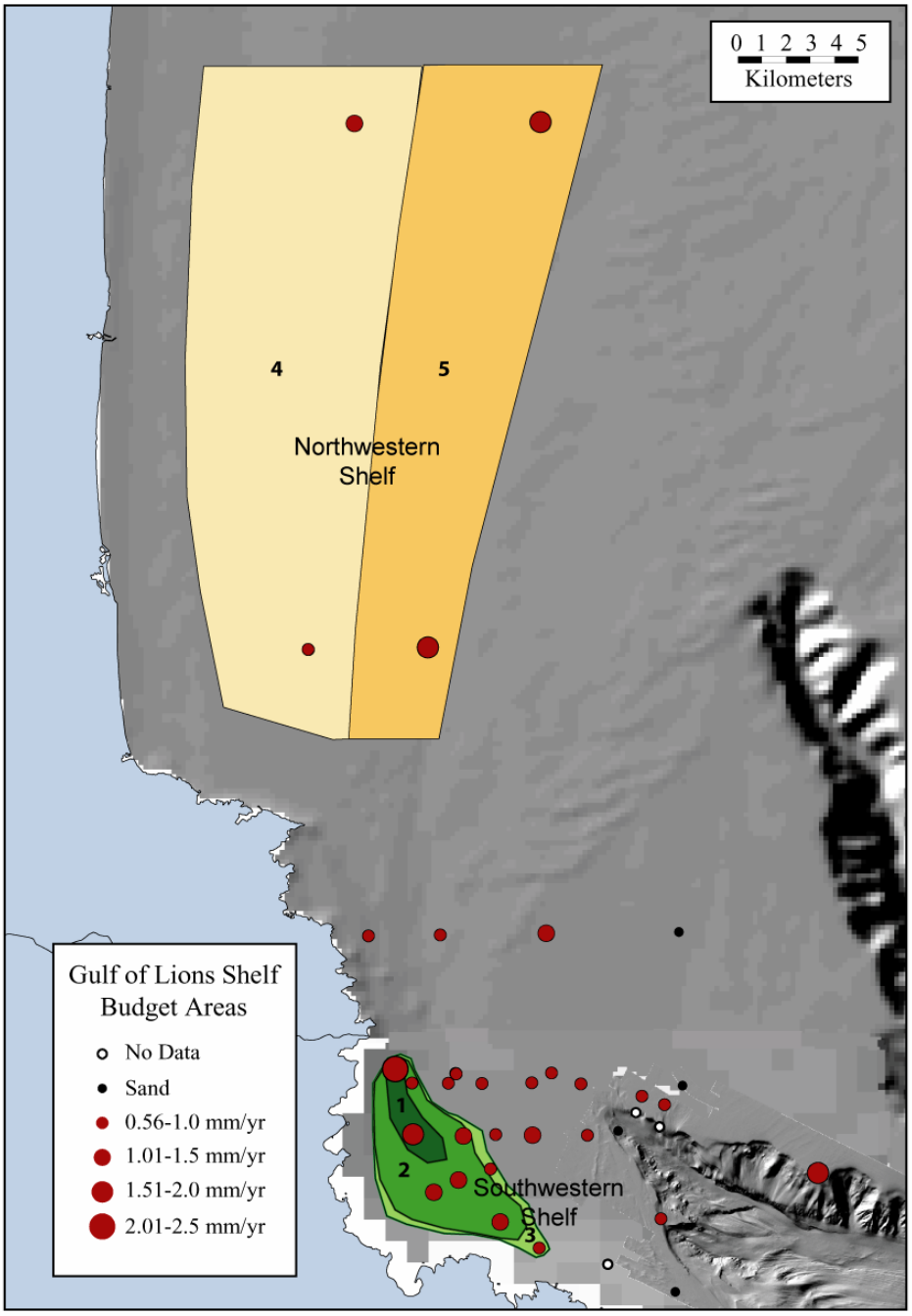

Figure 21. Shelf budget areas. The southwestern shelf calculations are based on areas 1, 2, and 3, while the northwestern shelf calculations use areas 4 and 5. Surface area was combined with bulk density and accumulation rates to determine total accumulation.

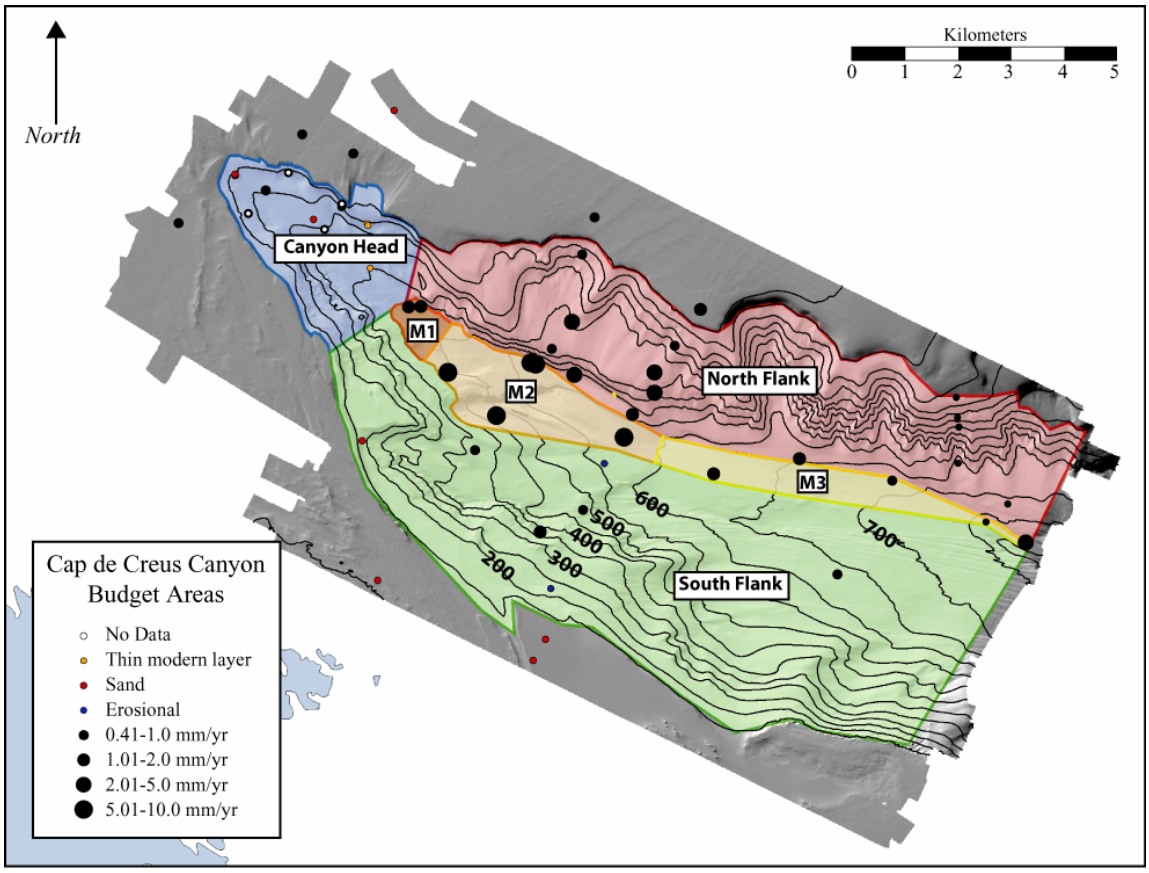

Figure 22. Canyon budget areas. The four regions used to calculate the canyon are shown by color: the canyon head, classified as non-depositional for fine-grains; the southern flank, also non-depositional; the northern flank, a depocenter for muds supplied by advection of nepheloid layers off the northern rim; and the mid-depth thalweg, location of the mud layer. The mud-layer was divided into three sections based on thickness and bulk-densities of sediments.

Table 5. Shelf budget calculations.

Section Number	*Area (m^2)*	*Mean Acc. Rate (mm/yr)*	*# of cores used*	*Standard deviation*	*Mean Bulk Density (g/cm^3)*	*Total Sediment (kg/yr)*	
Southwestern Shelf							
1	4.86×10^6	2.0	2	n/a	0.951 ± 0.15	$(9.24 \pm 3.3) \times 10^6$	
2	2.21×10^7	1.1	5	0.19	1.013 ± 0.13	$(2.55 \pm 0.54) \times 10^7$	
3	5.71×10^6	0.8	2	n/a	1.224 ± 0.20	$(5.73 \pm 1.3) \times 10^6$	
						$(4.04 \pm 1.0) \times 10^7$	kg sed. $year^{-1}$
						$(4.04 \pm 1.0) \times 10^4$	metric tons sed. $year^{-1}$
Northwestern Shelf							
4	2.20×10^8	1.1	2	n/a	0.953 ± 0.18	$(2.31 \pm 0.64) \times 10^8$	
5	1.65×10^8	2.0	2	n/a	0.906 ± 0.14	$(2.99 \pm 0.49) \times 10^8$	
						$(5.3 \pm 0.56) \times 10^8$	kg sed. $year^{-1}$
						$(5.3 \pm 0.56) \times 10^5$	metric tons sed. $year^{-1}$

Table 6. Canyon budget calculations

Section	*Surface Area* (m^2)	*Ave. Accum. Rate* (mm/yr)	*Cores used*	*Standard Deviation*	*Ave. Bulk Density* (g/cm^3)	*Total Sediment* (kg/yr)	
North Flank							
N/A	3.33×10^7	2.0	5	1.4	0.892 ± 0.18	$(5.97 \pm 4.4) \times 10^7$	kg sed. $year^{-1}$
						$(5.97 \pm 4.4) \times 10^4$	metric tons sed. $year^{-1}$

Section	*Surface Area* (m^2)	*Thick-ness* (m)	*Cores used*	*Standard deviation*	*Ave. Bulk Density* (g/cm^3)	*Total Sediment* (kg/ 22 yrs)	
Mud Layer							
1	7.39×10^5	0.045	2	N/A	0.760 ± 0.11	$(2.53 \pm 0.46) \times 10^7$	kg sed. (22 $years)^{-1}$
2	5.27×10^6	0.14	5	0.005	0.723 ± 0.12	$(5.34 \pm 0.91) \times 10^8$	
3	3.56×10^6	0.05	3	0.01	0.745 ± 0.20	$(1.33 \pm 0.45) \times 10^8$	
						$(6.9 \pm 1.4) \times 10^5$	metric tons sed. per 22 years
						$(3.1 \pm 0.64) \times 10^4$	metric tons sed. per year

Within the Cap de Creus canyon, the canyon head and most of the southern flank were classified as non-depositional areas and were given values of 0 tons of sediment input (considering fine-sediment deposition only). The northern flank was classified as a depositional area and was calculated to accrue $(5.97 \pm 4.4) \times 10^4$ tons of sediment annually (Table 6). The thalweg (from 400-780 m water depth) and a small portion of the surrounding flank (the near-thalweg southern flank) were classified as the mud layer. Overall, the entire layer was found to have $(69 \pm 14) \times 10^4$ tons of sediment (Table 6). Although it is only definitively known that this layer accumulated in less than 22 years, for the purpose of this annual budget, the total mass will be divided by 22 to determine an average annual input value. Using this method, a minimum value of $(3.1 \pm 0.64) \times 10^4$ tons of sediment is deposited annually in this layer. In total, an average of $(9.1 \pm 4.5) \times 10^4$ tons of sediment are deposited in Cap de Creus upper canyon annually.

Comparing these values with the total sediment input to the Gulf of Lions will allow for a better understanding of the relative importance of the western region. As good input-data are not available for the western rivers, comparisons are done using the Rhone sediment influx ($2.2\text{-}5 \times 10^6$ tons/year) and a rough estimate for the total influx to the Gulf, assuming the Rhone makes up 80% of the total (Zuo et al., 1999). These estimates are done using quantitative data from Got and Aloisi (1990) and Zuo et al (1999). To determine these values, the total mass accumulated for each region (shelf or canyon) is compared to the low (2.2×10^6 for the Rhone, 2.75×10^6 total) and high (5.0×10^6 for the Rhone only, 6.25×10^6 total) estimates of sediment input.

Based on the sediment input values to the Gulf of Lions, this study indicates that 11 – 29% of the Rhone input (9 – 23% of the total sediment influx) is sequestered on the southwestern portion of the Gulf of Lions shelf each year (Table 7). This verifies that there is significant transport and accumulation of sediment to the western portion of the Gulf of Lions continental shelf.

Within the canyon, this study indicates that 2 - 5% of the Rhone input (1 – 4% of the total sediment input) is sequestered in Cap de Creus upper canyon each year; this is an average over longer than a 100-year timescale and does not account for shorter timescale variability (Table 8). While these numbers seem small, it is important to note that they do not include sediment that passes rapidly through the canyon (such as may occur with the ephemeral mud layer, which annually stores over half the mass that is permanently deposited on the northern flank), only what is actually deposited within the thalweg and northern flank. Based on the high SSCs recorded by the mooring instruments (Fig. 19), it is likely that much more sediment actually passes through the canyon annually, but are not included in the total sediment budget for the upper canyon. On-going studies by Nittrouer and Lomnicky at locations deeper in the canyon (past this study area) will help constrain the total amount of sediment moving through Cap de Creus canyon.

Table 7. Comparison of shelf budget data with Rhone output.

Rhone	**Sed. discharge (tons/yr)**	**Southwestern Shelf (% of value)**	**Northwestern Shelf (% of value)**	**Total Western Shelf (% of value)**
Low estimate*	2.2×10^6	1.84	24.1	25.9
High estimate	5.0×10^6	0.81	10.6	11.4
Total Sediment (assuming Rhone is 80%)				
Low estimate	2.75×10^6	1.47	19.3	20.7
High estimate	6.25×10^6	0.65	8.5	9.13

* Estimates from Got and Aloisi (1990) and Zuo et al (1999).

Table 8. Comparison of canyon budget data with Rhone output.

Rhone	**Sed. discharge (tons/yr)**	**North Flank (% of value)**	**Mud Layer (% of value)**	**Upper Canyon (% of value)**
Low estimate*	2.2×10^6	3.0	1.4	4.4
High estimate	5.0×10^6	1.2	0.63	1.8
Low estimate	2.75×10^6	2.4	1.1	3.5
High estimate	6.25×10^6	0.95	0.50	1.4

* Estimates from Got and Aloisi (1990) and Zuo et al (1999).

5.5 Implications for Sediment Export During Sea-Level Highstands

This study has shown Cap de Creus upper canyon to be an important, preferential conduit of sediment to the deeper canyon and slope. Further, we have shown that while little sediment is accumulating (on 100-year timescales) within the upper canyon, significant amounts of sediment are passing through the canyon due to the unique oceanographic (dense-water cascading, current interactions with coastal morphology/bathymetry) and geologic (narrow shelf, canyon incision) conditions. Therefore, Cap de Creus canyon is ideally situated to move sediment off the continental shelf, despite its presence on a passive margin during a sea level highstand. The western Gulf of Lions, as a result, has a good combination of characteristics allowing off-shelf sediment export, even during sea-level high-stands.

This margin therefore has implications for the study of sediment-export from passive margins during sea-level highstands. The assumption that sediments are primarily trapped on these broad-shelves can be complicated by oceanographic conditions facilitating the movement of sediment over specific pathways. As such, an understanding of these conditions also affects our interpretation of deposits suspected of occurring during sea-level lowstands, which may actually instead have been influenced the right combination of factors allowing off-shelf sediment export during high-stands in sea level.

6. SUMMARY AND CONCLUSIONS

Accumulation rates and grain-size patterns reveal multiple depocenters on the Gulf of Lions western margin. On the shelf, fine sediment appears to be primarily accumulating at mid-shelf water depths on the northwestern section, and in a coastal "bulge" on the southwestern section. Within the canyon, the northern flank and mid-depth thalweg are modern depocenters (for fine-grained sediments). The canyon head and southern flank are considered non-depositional for fine grains, although the head may be accumulating coarse-grained material.

The pathways of sediment movement along the shelf and conduits of sediment into the canyon are variable (Fig. 23). Sediment that is not deposited on the northwestern shelf moves southward along the shelf to be deposited on the southwestern shelf or deflected around Cap de Creus headland. Material enters the canyon from the northern rim (via advection of shelf benthic nepheloid layers), the southern rim (via dense-water cascading off the shelf), and through the canyon head (primarily coarse-grains, definitive mechanism unknown).

Overall, Cap de Creus canyon is an important area of sediment export from the Gulf of Lions continental shelf. However, rather than acting as a sediment trap, it functions as a funnel, moving sediment from the shelf region towards deeper water. This study indicates that sediment can escape the shelf of a passive margin (despite the present sea-level highstand and location distal to fluvial sources) due to regional circulation patterns and topographic steering, both of which can have strong influences on sediment export past the shelf break.

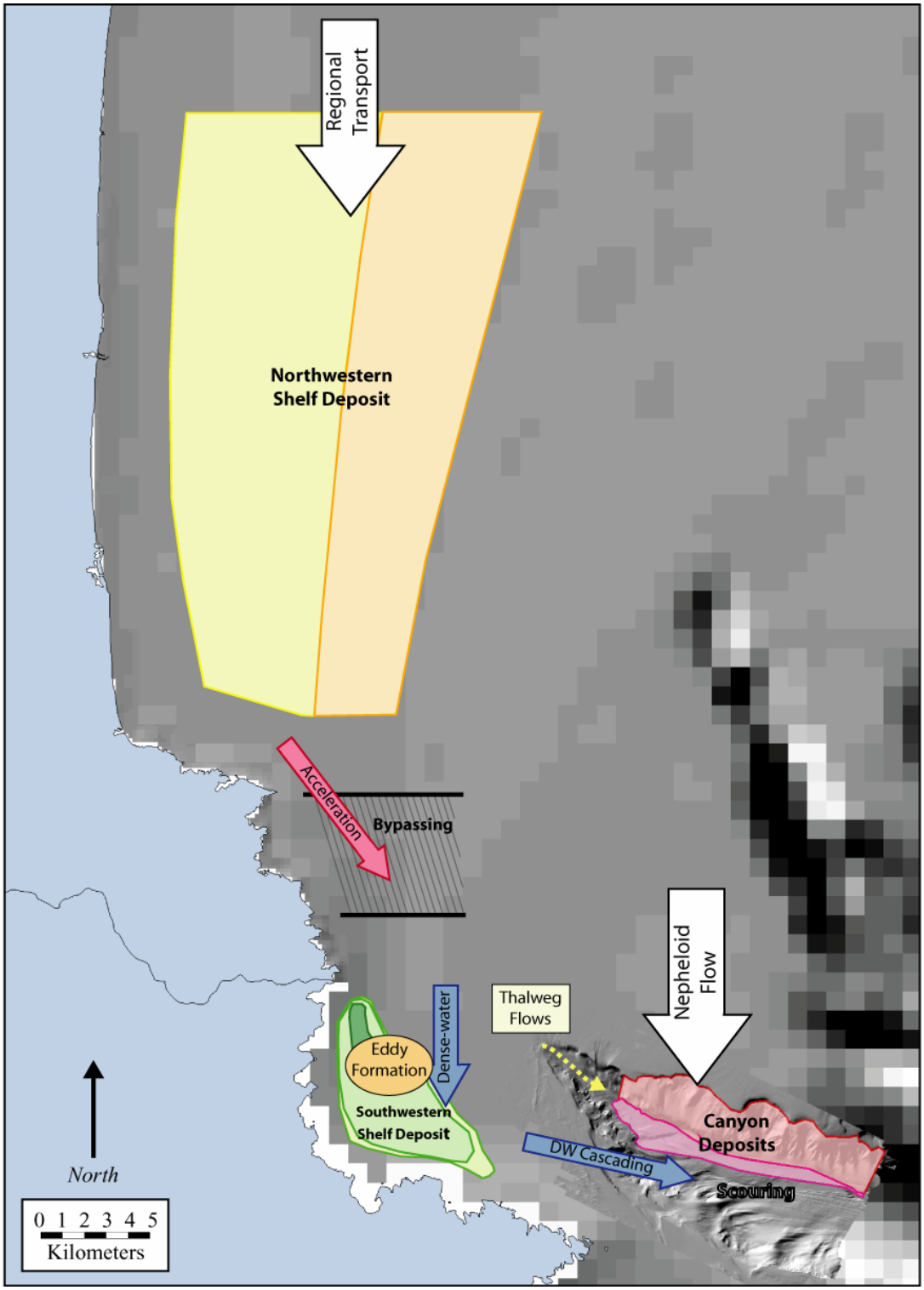

Figure 23. Summary schematic diagram of depocenters, pathways, and processes.

REFERENCES

Arnau, P., Liquete, C., Canals, M., 2004. River mouth plume events and their dispersal in the Northwestern Mediterranean Sea. Oceanography 17, 22-31.

Baker, E.T., Hickey, B.M., 1986. Contemporary sedimentation processes in and around an active west coast submarine canyon. Marine Geology 71, 15-34.

Baztan, J., Berne, S., Olivet, J.L., Rabineau, M., Aslanian, D., Gaudin, M., Rehault, J.P., Canals, M., 2005. Axial incision: the key to understand submarine canyon evolution (in the western Gulf of Lion). Marine and Petroleum Geology 22, 805-826.

Baztan, J., Berne, S., Olivet, J.L., Rabineau, M., Aslanian, D., 2004. A key to understand submarine canyon evolution in the Gulf of Lion (Mediterranean Sea). AGU Fall Meeting, San Francisco, California, December 13-17.

Berne, S., Gorini, C., 2005 The Gulf of Lions: an overview of recent studies within the French Margins programme. Marine and Petroleum Geology 22, 691-693.

Berne, S., M. Rabineau, J.A. Flores, and F.J. Sierro. 2004. The impact of Quaternary global changes on strata formation: exploration of the shelf edge in the northwest Mediterranean Sea. Oceanography 17, 92-103.

Berne, S., Aloisi, J.C., Baztan, J., Dennielou, B., Droz, L., Dos Reis, T., Lofi, J., Mear, Y., Rabineau, M., Satra, C., 2002. Notice de la carte morpho-bathymetrique du Gulf du Lion. IFREMER et Region Langeudoc Roussillon, Brest.

Bettoli, M.G., Cantelli, L., Degetto, S., Tositti, L., Tubertini, O., Valcher, S., 1995. Preliminary investigations on ^{7}Be as a tracer in the study of environmental processes. Journal of Radioanalytical and Nuclear Chemistry Articles 190, 137-147.

Boggs, S. Jr. 2001. Principles of Sedimentology and Stratigraphy. Prentice Hall. Upper Saddle River, New Jersey.

Broecker, W.S., Turekian, K.K., Heezen, B.C., 1958. The relation of deep sea sedimentation rates to variations in climate. American Journal of Science 256, 503-517.

Canals, M., Casamor, J.L., Lastras, G., Monaco, A., Acosta, J., Berne, S., Loubieu, B., Weaver, P.P.E., Grehan, A., Dennielou, B., 2004. The role of canyons in strata formation. Oceanography 17, 80-91.

Carson, B., Baker, E.T., Hickey, B.M., Nittrouer, C.A., DeMaster, D.J., Thorbjarnarson, K.W., Snyder, G.W., 1986. Modern sediment dispersal and accumulation in Quinault submarine canyon – a summary. Marine Geology 71, 1-13.

Certain, R., Tessier, B., Barusseau, J.P., Courp, T., Pauc, H., 2005. Sedimentary balance and sand stock availability along a littoral system. The case of the western Gulf of Lions littoral prism (France) investigated by very high resolution seismic. Marine and Petroleum Geology 22, 889-900.

Courp, T., Monaco, A., 1990. Sediment dispersal and accumulation on the continental margin of the Gulf of Lions: sedimentary budget. Continental Shelf Research 10,1063-1087.

Davies, P.A., Dakin, J.M., Flaconer, R.A., 1995. Eddy formation behind a coastal headland. Journal of Coastal Research 11, 154-167.

Durrieu de Madron, X., 2005. Personal Communication.

Durrieu de Madron, X., Zervakis, V., Theocharis, A., Georgopoulos, D., 2005. Comments on "Cascades of dense water around the world ocean". Progress in Oceanography 64, 83-90.

Durrieu de Madron, X. 2004. Cold-water outbreaks on the Gulf of Lions continental margin. AGU Fall Meeting. San Francisco, California, December 13-17.

Durrieu de Madron, X. 1994. Hydrography and nepheloid structures in the Grand-Rhone canyon. Continental Shelf Research 14, 457-477.

Durrieu de Madron, X., Nyffeler, F., Godet, C.H., 1990. Hydrographic structure and nepheloid spatial distribution in the Gulf of Lions continental margin. Continental Shelf Research 10, 915-929.

Emery, K.O. 1968. Relict sediments on continental shelves of the world. American Association of Petroleum Geologists Bulletin, 445-464.

Field, M., Hart, P., 2005. Personal communication.

Frignani, M., Courp, T., Cochran, J.K., Hirshberg, D., Vitoria Codina, L., 2002. Scavenging rates and particle characteristics in and near the Lacaze-Duthiers submarine canyon, northwest Mediterranean. Continental Shelf Research 22, 2175-2190.

Fukushima, Y., Parker, G., Pantin, H.M., 1985. Prediction of ignitive turbidity currents in Scripps submarine canyon. Marine Geology 67, 55-81.

Gardner, W.D. 1989. Baltimore canyon as a modern conduit of sediment to the deep sea. Deep-Sea Research 36, 323-358.

Geyer, W.R. 1993. Three-dimensional tidal flow around headlands. Journal of Geophysical Research 98, 955-966.

Geyer, W.R., Signell, R., 1990. Measurements of tidal flow around a headland with a shipboard acoustic doppler current profiler. Journal of Geophysical Research 95: 3189-3197.

Got, H., Aloisi, J.C., 1990. The Holocene sedimentation on the Gulf of Lions margin: a quantitative approach. Continental Shelf Research 10, 841-855.

Granata, T.C., Vidondo, B., Duarte, C.M., Satta, M.P., Garcia, M., 1999. Hydrodynamics and particle transport associated with a submarine canyon off Blanes (Spain), NW Mediterranean Sea. Continental Shelf Research 19, 1249-1263.

Hickey, B., Baker, E., Kachel, N., 1986. Suspended particle movement in and around Quinault submarine canyon. Marine Geology 71, 35-83.

Jago, C.F., Barusseau, J.P., 1981. Sediment entrainment on a wave-graded shelf, Roussillon, France. Marine Geology 42, 279-299.

Kineke, G.C., Woolfe, K.J., Kuehl, S.A., Milliman, J.D., Dellapenna, T.M., Purdon, R.G., 2000. Sediment export from the Sepik River, Papua New Guinea: evidence for a divergent sediment plume. Continental Shelf Research 20, 2239-2266.

Larsen, I.L., Cutshall, N.H., 1981. Direct determination of ^{7}Be in sediments. Earth and Planetary Science Letters 54, 379-384.

Liu, J.T., Liu, J., Huang, J.C., 2002. The effect of a submarine canyon on the river sediment dispersal and inner shelf sediment movements in southern Taiwan. Marine Geology 181, 357-386.

Martin, J.M., Elbaz-Poulichet, F., Guieu, C., Loye-Pilot, M.D., Han, G., 1989. River versus atmospheric input of material to the Mediterranean Sea: an overview. Marine Chemistry 28, 159-182.

Martin, R.T., Gadel, F.Y., Barusseau, J.P., 1981. Holocene evolution of the Canet-St. Nazaire lagoon (Golfe du Lion, France) as determined from a study of sediment properties. Sedimentology 28, 823-836.

Miller, M.C., McCave, I.N., Komar, P.D., 1977. Threshold of sediment motion under unidirectional currents. Sedimentology 24, 507-527.

Milliman, J.D., Syvitski, J.P.M., 1992. Geomorphic/tectonic control of sediment discharge to the ocean: the importance of small, mountainous rivers. The Journal of Geology 100, 525-544.

Milliman, J.D., Meade, R.H. 1983. World-wide delivery of river sediment to the oceans. The Journal of Geology 91, 1-21.

Millot, C. 1990. The Gulf of Lions hydrodynamics. Continental Shelf Research 10, 885-894.

Monaco, A., Durrieu de Madron, X., Radakovitch, O., Heussner, S., Carbonne, J., 1999. Origin and variability of downward biogeochemical fluxes on the Rhone continental margin (NW Mediterranean). Deep-Sea Research I 46, 1483-1511.

Mullenbach, B.L. Nittrouer, C.A., Puig, P., Orange, D.L., 2004. Sediment deposition in a modern submarine canyon: Eel Canyon, northern California. Marine Geology 211, 101-119.

Mullenbach, B.L., 2002. Characterization of modern off-shelf sediment export on the Eel margin, northern California. PhD Dissertation. University of Washington, WA, 154 pp.

Mullenbach, B.L., Nittrouer. C.A., 2000. Rapid deposition of fluvial sediment in the Eel Canyon, northern California. Continental Shelf Research 20, 2191-2122.

Nittrouer, C.A., 1999. STRATAFORM: overview of its design and synthesis of its results. Marine Geology 154**,** 3-12.

Nittrouer, C.A., Kravitz, J.H. 1996. STRATAFORM: a program to study the creation and interpretation of sedimentary strata on continental margins. Oceanography 9, 146-157.

Nittrouer, C.A., Wright, L.D., 1994. Transport of particles across continental shelves. Reviews of Geophysics 32, 85-113.

Nittrouer, C.A., Sternberg, R.W., 1981. The formation of sedimentary strata in an allocthonous shelf environment – the Washington Continental Shelf. Marine Geology 42, 201-232.

Nittrouer, C.A., Sternberg, R.W., Carpenter, R., Bennett, J.T., 1979. The use of ^{210}Pb geochronology as a sedimentological tool: application to the Washington continental shelf. Marine Geology 31, 297-316.

Olsen, C.R., Larsen, I.L., Lowry, P.D., Cutshall, N.H., Todd, J.F., Wong, G.T.F., Casey, W.H., 1985. Atmospheric fluxes and marsh-soil inventories of ^{7}Be and ^{210}Pb. Journal of Geophysical Research 90, 10,487-10,495.

Paull, C.K., Mitts, P., Ussler III, W., Keaten, R., Greene, H.G., 2005. Trail of sand in upper Monterey Canyon: offshore California. Geological Society of America Bulletin, 117: 1134-1145.

Paull, C.K., Ussler III, W., Greene, H.G., Keaton, R., Mitts, P., Barry, J., 2003. Caught in the act: the 20 December 2001 gravity flow event in Monterey Canyon. Geo-Marine Letters 22, 227-232.

Pawlak, G., MacCready, P., 2002. Oscillatory flow across an irregular boundary. Journal of Geophysical Research 107, 1-17.

Puig, P., 2005. Personal Communication.

Puig, P., Ogston, A.S., Mullenbach, B.L., Nittrouer, C.A., Parsons, J.D., Sternberg, R.W., 2004. Storm-induced gravity flows at the head of the Eel submarine canyon, northern California Margin. Journal of Geophysical Research 109, C03019.

Puig, P., Palanques, A., 1998. Temporal variability and composition of settling particle fluxes on the Barcelona continental margin (Northwestern Mediterranean). Journal of Marine Research 56, 629-654.

Sanchez-Cabeza, J.A., Masque, P., Ani-Ragolta, I., Merino, J., Frignani, M., Alvisi, F., Palanques, A., Puig, P., 1999. Sediment accumulation rates in the southern Barcelona continental margin (NW Mediterranean Sea) derived from ^{210}Pb and ^{137}Cs chronology. Progress in Oceanography 44, 313-332.

Signell, R.P., Harris, C.K., 2000. Modeling sand bank formation around tidal headlands, *in* Estuarine and Coastal Modeling, 6th Int. Conf., ASCE, New Orleans, November 3-5, 1999. Editors: M.L. Spaulding and A.F. Blumberg.

Sommerfield, C.K., Nittrouer, C.A., 1999. Modern accumulation rates and a sediment budget for the Eel Shelf: a flood-dominated depositional environment. Marine Geology 154, 227-241.

Sommerfield, C.K., Nittrouer, C.A., Alexander, C.R., 1999. Be-7 as a tracer of flood sedimentation on the northern California continental margin. Continental Shelf Research 19, 355-361.

Snyder, G.W., Carson, B., 1986. Bottom and suspended particle sizes: implications for modern sediment transport in Quinault Submarine Canyon. Marine Geology 71, 85-105.

Thorbjarnarson, K.W., Nittrouer, C.A., DeMaster, D.J., 1986. Accumulation of modern sediment in Quinault Submarine Canyon. Marine Geology 71, 107-124.

Walsh, J.P., Nittrouer., C.A., 2003. Contrasting styles of off-shelf accumulation in New Guinea. Marine Geology 196, 105-125.

Wegrzynek, D., Jambers, W., Van Grieken, R., Eisma, D., 1997. Individual particle analysis of western Mediterranean sediment cores, Rhone suspended matter and Sahara aerosols – investigation of inputs to the sediments. Marine Chemistry 57, 41-53.

Zuo, Z., Eisma, D., Gieles, R., Beks, J., 1997. Accumulation rates and sediment deposition in the northwestern Mediterranean. Deep-Sea Research II 44, 597-609.

Zuo, Z., Eisma, D., Berger, G.W., 1991. Determination of sediment accumulation and mixing rates in the Gulf of Lions, Mediterranean Sea. Oceanologica Acta 14, 253-262.

VITA

Amy Louise DeGeest graduated from the University of Washington in August of 2003 with a Bachelor of Science in oceanography (*cum laude)* and a Bachelor of Science in geological sciences. Her senior thesis was: Sediment response to airborne pollutants in Lake Washington. She earned a Master of Science in oceanography (geological section) from Texas A&M University, College Station in December 2005. Her research focused primarily on modern marine sedimentation as a part of the ONR-funded EuroSTRATAFORM project.

Ms. DeGeest can be reached at 3503 103rd Place SE, Everett, Washington 98208 or via email at amydegeest@hotmail.com.